Beat-to-Beat Estimation of Blood Pressure by Artificial Neural Network

By:

Azadeh Dastmalchi

A thesis submitted to the

Faculty of Graduate and Postdoctoral Studies

In partial fulfillment of the requirements for the degree of

Master of Applied Science in Biomedical Engineering

Department of Mechanical Engineering

Faculty of Engineering

University of Ottawa

ABSTRACT

High blood pressure is a major public health issue. However, there are many physical and non-physical factors that affect the measurement of blood pressure (BP) over very short time spans. Therefore, it is very difficult to write a mathematical equation which includes all relevant factors needed to estimate accurate BP values. As a result, a possible solution to overcome these limitations is the use of an artificial neural network (ANN). The aim of this research is to design and implement a new ANN approach, which correlates the arterial pulse waveform shape to BP values, for estimation of BP in a single heartbeat. To test the feasibility of this approach, a pilot study was performed on an arterial pulse waveform dataset obtained from 11 patients with normal BP and 11 patients with hypertension. It was found that the proposed method can accurately estimate BP in single heartbeats and satisfy the requirements of the ANSI/AAMI standard for non-invasive measurement of BP.

Keywords: arterial pulse waveform, blood pressure, artificial neural network

Acknowledgments

It is my pleasure to thank the many people who made this research possible, first and foremost my family. My thanks go to my husband, Soroosh, my beloved parents, Kezam and Hamideh, and my dear parents-in-law for their understanding, patience, and encouragement during the period of my graduate studies. I am also grateful to my brother Mohammad Reza for his help in drawing most of the graphics in this thesis. I should also thank my sister-in-law, Nafiseh Moshir Ehteshami, who took care of editing the last draft of this thesis.

I wish to express my most sincere appreciation to Dr. Hilmi R. Dajani for his supervision, constant support, and his constructive comments throughout the development of the project. The work could also not have been completed without the aid of my colleague Dr. Mohamad Forouzanfar. It has been a pleasure collaborating with each member of this team.

I would also like to thank and acknowledge my previous supervisor Professor Tofy Mussivand, his lab manager Mr. Kevin Holmes, postdoctoral fellows Dr. Armin Sabri and my lab mate John Szalas, my friends Alireza Sadr, Mohammad Faraji and Omid Gheibi who have been of invaluable assistance when I hit a bottleneck during the period of completing this project.

I wish to express my last, but not least, wholehearted thanks to my friends Mana Shahirari, Fahimeh Soleymani, Zahra Zangenehmadar, Helyeh Doutaghi, Mohammad Mahdi Gharaeemanesh, Masoumeh Mirzaee and her family, for their motivation, encouragement and support.

Contents

List of Figures

List of Tables

List of Abbreviations

AAMI: Association for the Advancement of Medical Instrumentation

ABP: Arterial Blood Pressure (signal)

ANN: Artificial Neural Network

ANSI: American National Standards Institute

BP: Blood Pressure

BPM: Blood Pressure Monitoring

bpm: beats per minute

BSN: Body Sensor Network

CO: Cardiac Output

***DBP*:** Diastolic Blood Pressure

***ECG*:** Electrocardiogram

EDV: End Diastolic Volume

ESV: End Systolic Volume

FF: Feed-Forward

FFNN: Feed-Forward Neural Network

HBP: High Blood Pressure or hypertension

HR: Heart Rate

***mmHg*:** millimeter of mercury

LR: Linear Regression

MAE: Mean Absolute Error

***MAP*:** Mean Arterial Pressure

ME: Mean Error

MLP: a multilayer perceptron

NN: Neural Network

PPG**:** Photoplethysmogram

PW**:** Pulse Wave

RF: Random Forest

SBP**:** Systolic Blood Pressure

SD: Standard Deviation

SDAE: Standard Deviation of Absolute Error

SDE: Standard Deviation of Error

SV: Stroke Volume

SVM: Support Vector Machine

1 Introduction

High blood pressure (hypertension) is a major public health issue [1]. It contributes to heart disease, stroke and kidney failure and premature mortality and disability. Globally, one-third of deaths are due to cardiovascular disease [2]. Hypertension is responsible for at least 45% of deaths due to heart disease and 51% of death due to stroke [2]. According to Hypertension Canada report, 25% of Canadians have hypertension [3]. Consequently, blood pressure monitoring (BPM) is necessary for diagnosis and management of various health conditions. There are two major groups of methods used for BPM: invasive and non-invasive. For invasive BPM, a patient usually has to be hospitalized, and a catheter that is inserted into the artery measures blood pressure (BP) directly. There are many methods for non-invasive blood pressure monitoring which are more convenient and carry few risks such as auscultatory, oscillometric, ultrasonic, unloaded vascular, tonometry, flush, and plethysmography, almost all of which use a cuff as part of the device [4]. The main issues with current BPM devices are that 1) the cuff is a demonstrable source of error due to considerations such as a patient's anxiety due to inflating the cuff, size incompatibility and improper installation, and 2) all BPM devices are limited in terms of applicability, i.e. we don't have a specific device to use for all populations such as pregnant women, children, the elderly, and obese patients [4]. Additionally, there are many physical and non-physical factors (e.g. emotional state and posture of a person) that affect BP values even within a few heartbeats [4]. Therefore, it is in practice not possible to write an analytic equation which includes all relevant factors for estimating BP accurately. As a result, a possible solution to overcome some of these limitations such as issues related to the cuff is the use of the Artificial Neural Network (ANN) which is able to relate outputs (BP estimates) and inputs (arterial pulse waveform data) without using an analytic formula. Moreover, by relying only on the morphology

of the arterial pulse waveform and not on its amplitude, the ANN may provide a way to implement cuffless BP estimation where the arterial pulse waveform is measured non-invasively using an appropriate sensor (such as a photoplethysmographic or tonometric sensor). In addition to eliminating discomfort due to the inflating cuff, a cuffless BP device is highly desirable clinically because it could allow tracking of BP changes continuously from beat to beat. Such a development would have a number of applications, including beat-to-beat BP estimation during surgery, in the intensive care unit (ICU), and during sleep.

The aim of this research study is to design and develop an ANN approach to estimating BP based on the arterial pulse shape. The arterial pulse wave samples were obtained from normalized invasive BP waveforms extracted from the online Multi-parameter Intelligent Monitoring in Intensive Care (MIMIC) database. To test the feasibility of the proposed method, the dataset used to train and test the ANN included 22 patients with 10 pulse periods each, of whom 11 patients have normal blood pressure and 11 patients have hypertension. A further set of 3 patients (2 with normal pressure and 1 with hypertension) with 10 pulse periods each, and with whom the ANN had no prior exposure, were also used to test the performance of the method. The accuracy of the BP estimates obtained with the proposed method was compared with the requirements of the ANSI/AAMI standard protocol for non-invasive BP devices.

Because the proposed method is ultimately intended to be implemented in the software of a cuffless BPM device, the computational complexity of the algorithms is one of the considerations of this research study. Therefore, a multilayer perceptron (MLP), feed-forward (FF) backpropagation is proposed for the ANN, which compared to other ANN architectures such as radial basis function, counter propagation, and learning vector quantization, requires a smaller number of neurons when the training set is large.

The structure of this thesis is as follows: Chapter 2 reviews the physiology of blood pressure, factors that affect blood pressures, methods and devices for blood pressure measurement which are currently available, and the current issues with these methods and devices. Chapter 3 describes the source of the data used in this work, how the pulse signal is selected, normalization, interpolation, and feature extraction from the raw signal, and the ANN structure that was used. Chapter 4 describes the performance of the proposed algorithm and compares the results with current BP measurement standards as well as with the results of other research groups. Chapter 5 summarizes the contributions of the thesis, limitations, and future work. A table showing the estimated and reference blood pressure values in each individual heartbeat analyzed in this study are provided in the appendix.

2 Literature Review

2.1 Background

Blood Pressure (BP) is a vital sign that is defined as the force that blood exerts against the wall of blood vessels [5, 6]. Measuring BP is important because it is a significant indicator of the health and function of an individual's cardiovascular system, as well as an independent risk factor for stroke, heart attack, blindness and renal diseases [5-9]. By measuring BP, hypertension can be detected early and treated with changes in lifestyle choices and/or medications to improve overall health before irreversible damage occurs to any of the relevant organs [5-9]. BP levels help physicians determine the functional integrity of the cardiovascular system [10], and they are typically expressed as the ratio of systolic and diastolic pressures. Systolic pressure is the maximum pressure in the arteries when the heart beats (ventricular contraction), while diastolic pressure is the minimum pressure in the arteries when the heart is at rest (ventricular relaxation), and they are both indicated in millimeters of mercury (mmHg). As shown in Table 2.1, Hypertension has three stages, the Pre-hypertension stage with the systolic value between 120 and 139 mmHg or diastolic value between 80 and 89 mmHg. Stage 1 Hypertension with systolic between 140 and 159 or diastolic between 90 and 99 ommHg, and Stage 2 Hypertension with systolic more than 160 mmHg or diastolic more than 100 mmHg. Based on the World Health Organization report in 2014, an estimated one fourth of adults worldwide were reported to suffer from hypertension [11]. It is precisely for this reason that regular monitoring of high blood pressure (HBP) is essential [5]. In addition, continuous blood pressure monitoring (BPM) would help in treating other diseases such as aneurysms and spinal cord injury [12].

Table 2.1 Blood pressure values (in mmHg) and stages.

Category	systolic		Diastolic
Normal	<120	And	<80
Pre-hypertension	120-139	Or	80-89
Hypertension Stage 1	140-159	Or	90-99
Hypertension Stage 2	>160	Or	>100

However, although determining BP is one of the most important measurements in all of the clinical medicine, it is still one of the most inaccurately performed. Accordingly, accurate measurement of BP is essential to classify individuals, predict outcomes, and diagnose and treat diseases correctly [6, 13, 14].

Blood pressure can be divided into two main categories: Pulmonary and Systemic BP. Pulmonary BP is the pressure that is applied in the pulmonary circulation, while systemic BP is the pressure that occurs in the systemic circulation. Systemic BP consists of central and peripheral parts. Central BP relates to locations close to the heart (e.g. in the aorta) while peripheral BP relates to locations away from the heart (usually in the limbs) [15].

This chapter introduces the current methods and devices used for measuring blood pressure, and discuss common issues and problems associated with them. It also reviews recent research on cuffless methods and devices for continuous BPM, that attempt to overcome some of these problems. Extravascular and intravascular sensors will be explored within the framework of

invasive techniques. Non-invasive methods such as the auscultatory and oscillometric methods and their devices will also be discussed.

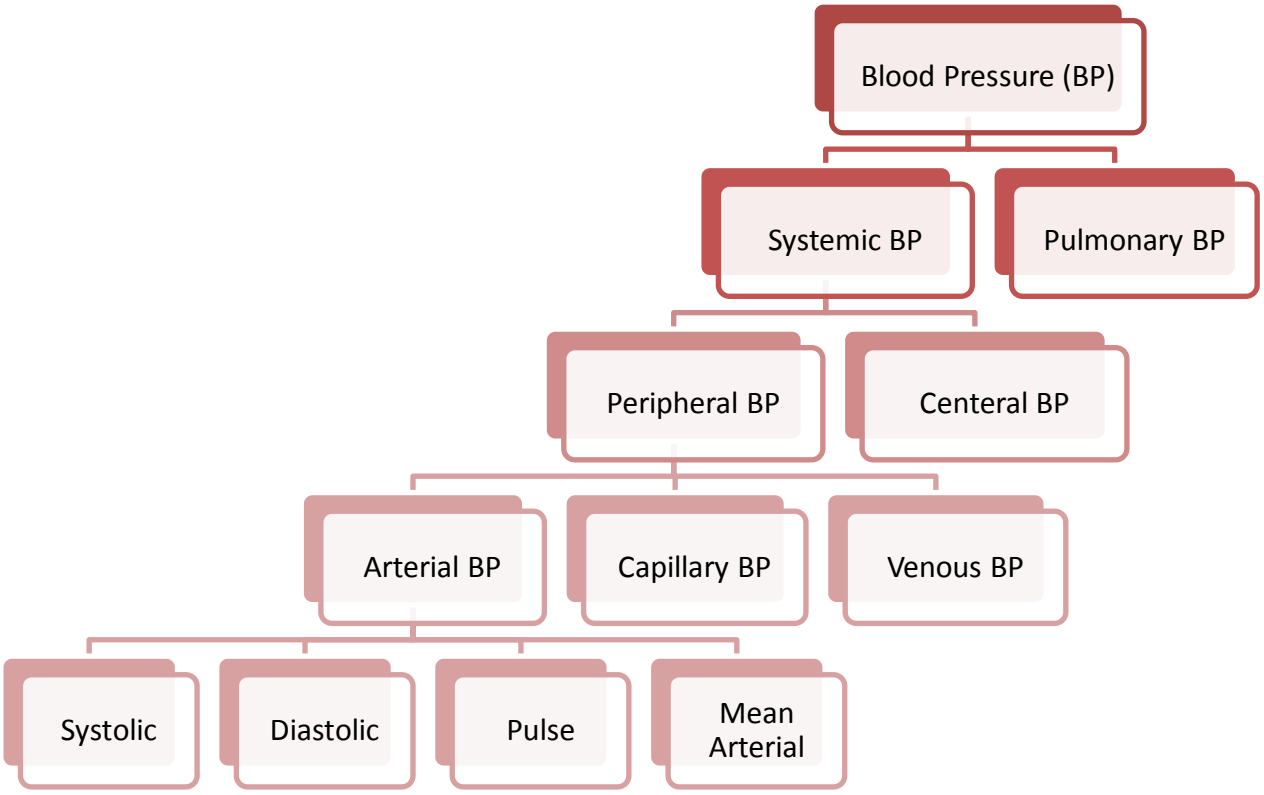

Figure 2.1 A flowchart of blood pressure divisions.

Figure 2.1 shows the types of blood pressure that are of interest. Since our study is not concerned with pulmonary, central, venous or capillary BP, we did not extend their parts in the graph. Figure 2.2 shows the division of peripheral blood pressure into three main groups: arterial pressure, which is pulsatile, capillary blood pressure and venous pressure, which are non-pulsatile. Peripheral arterial blood pressure is the quantity that is usually measured [5].

Therefore, blood pressure refers to the measure of systolic and diastolic pressure in peripheral arterial vessels (typically in the upper arm or in the wrist).

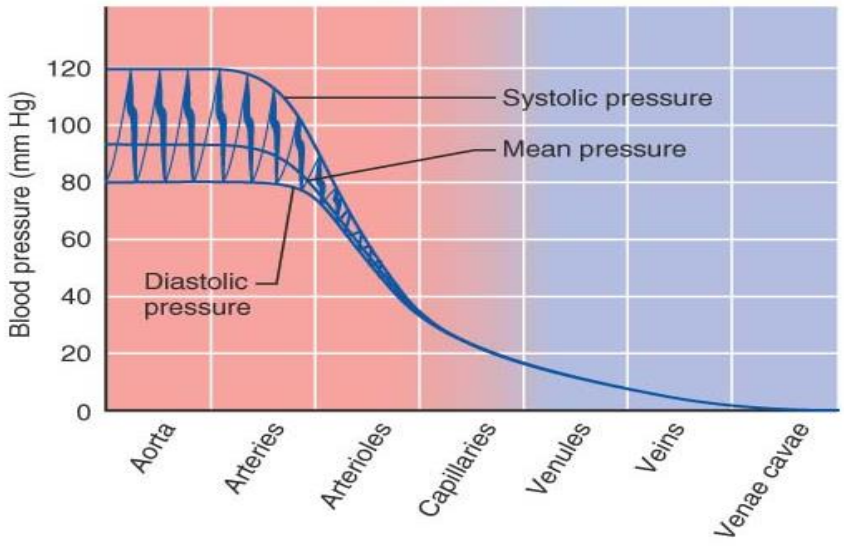

Figure 2.2 Systemic Blood Pressure (adapted from [5]).

The arterial pulse wave, as shown in Figure 2.3, is a signal which can be characterized by different components such as 1) Systolic BP, 2) Diastolic BP, 3) Pulse Pressure, 4) Mean Arterial Pressure (MAP), and 5) Dicrotic Notch. Systolic pressure is the peak during systole. The diastolic pressure occurs during diastole, as blood is forced distally in the circulatory system by the rebound of elastic arteries, and arterial BP drops to its lowest value. The difference between systolic and diastolic pressure is called pulse pressure.

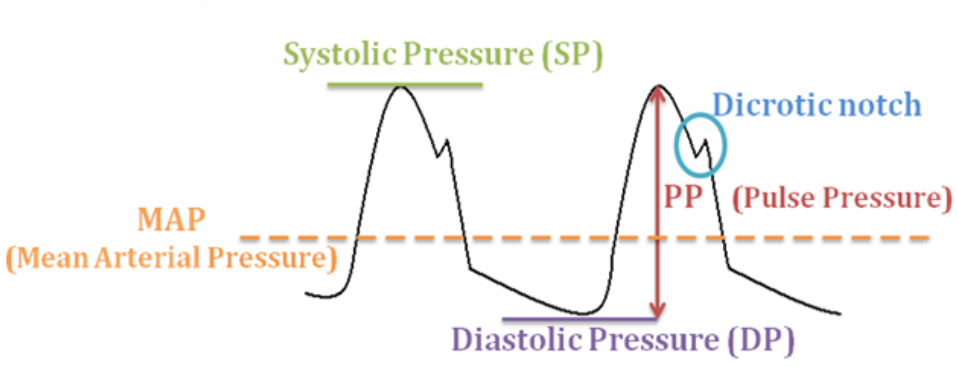

Figure 2.3 Arterial pulse wave and its components.

The Mean Arterial Pressure (MAP) is the force that propels blood through the arteries. It is calculated as "average" pressure in the arteries during the pulse, and since the heart stays longer in diastole, MAP is closer to the diastolic pressure than systolic pressure and is not equal to the algebraic average of the two. At normal heart rates, it can be approximated by the following equation:

$$\text{Mean Arterial Pressure (MAP)} = \text{Diastolic Pressure} + 1/3\ \text{Pulse Pressure} \quad (2.1)$$

2.2 Factors Influencing Blood Pressure

There are many factors that affect blood pressure, which may be grouped into the two following categories: a) “internal” physiological factors, b) other factors. The physiological factors that affect blood pressure are summarized in Figure 2.4 and include peripheral resistance (PR), vessel elasticity (VE), stroke volume (SV) and cardiac output (CO). Other factors influencing BP include body posture, crossing legs, age, sex, pain, smoking, obesity, alcohol, stress, and anxiety [7].

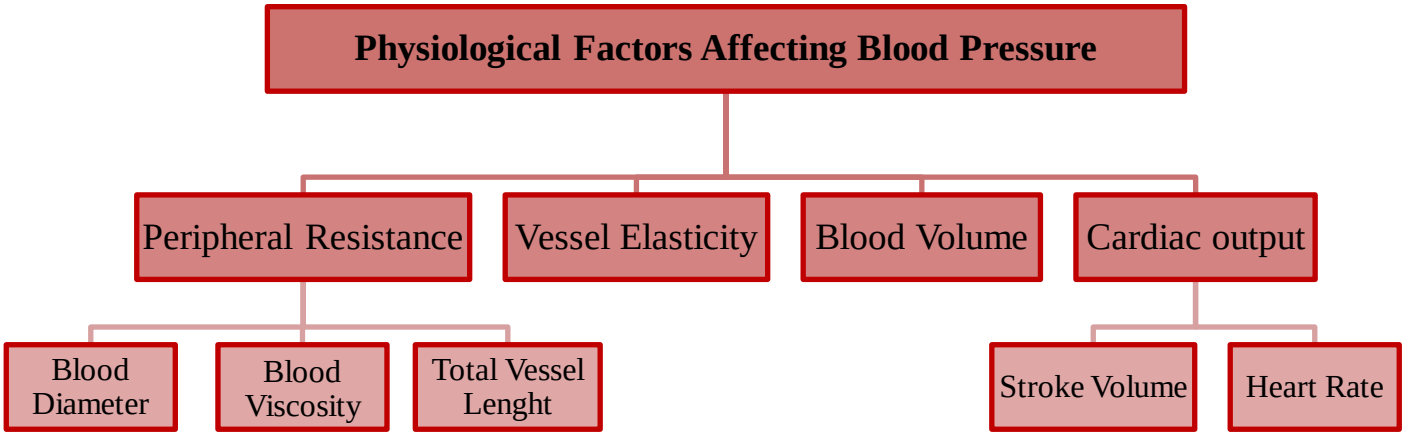

Figure 2.4 Physiological factors that affect blood pressure.

2.2.1 Stroke Volume (SV)

Stroke volume depends on the degree of stretch of cardiac muscle by venous return and is equal to the difference between end diastolic volume (EDV) and end systolic volume (ESV) or approximately 70 ml [5].

$$SV = EDV - ESV \qquad (2.2)$$

Anything that influences heart rate or blood volume influences venous return, and hence stroke volume. If less blood is pumped from the heart with each beat, then blood pressure will be lower because there is less blood pressing against the vessel walls. Blood volume directly affects end diastolic volume (EDV) and stroke volume.

2.2.2 Cardiac Output (CO)

Cardiac output is the amount of blood pumped out by each ventricle in one minute. Cardiac output is directly proportional to the blood pressure. Average CO for resting healthy male is equal to 5 L/min [5].

$$CO = HR \times SV \qquad (2.3)$$

where CO = cardiac output, HR = heart rate, and SV = stroke volume

2.2.3 Heart Rate (HR)

Heart rate is the number of heart beats per minute (bpm). The normal resting heart rate for an adult is around 75 bpm. As shown in Figure 2.4, there are several factors that influence heart rate directly such as sympathetic, parasympathetic and chemical regulation [5].

2.2.4 Blood Volume

Blood volume directly affects blood pressure [5]. A greater volume of fluid presses against the walls of the arteries resulting in greater sustained pressure. Accordingly, a lower volume of fluid results in less pressure [5].

2.2.5 Vessel Elasticity

Blood vessel elasticity also affects blood pressure [5]. A healthy elastic artery expands and absorbs the shock of systolic pressure. The elastic recoil of the vessel maintains the continued flow of blood during diastole. An individual with arteriosclerosis suffers from calcified and rigid arteries, preventing them from expanding as the pulse wave of systolic pressure passes through the arteries. Consequently, the walls of the artery sustain higher pressures and become weaker.

2.2.6 Peripheral Resistance

One of the main factors that affect blood pressure is peripheral resistance [5]. Blood cells and plasma encounter resistance when they come into contact with blood vessel walls. If resistance increases, more pressure is needed to keep blood flowing. Three main sources of peripheral resistance are, blood vessel diameter, blood viscosity, and total vessel length, which can be formulated as below [5]:

$$R=\frac{8L\eta}{\pi r^4} \qquad (2.4)$$

where η= viscosity, L= length of a blood vessel, r= inside radius of a blood vessel

2.2.7 Blood Viscosity

The hematocrit is the percentage of red blood cells in the total blood volume. It affects blood viscosity and resistance to flow. The more viscous the blood, the greater resistance it encounters and the higher the blood pressure. The opposite holds true as well [5].

2.2.8 Vessel Length

Total vessel length directly affects peripheral resistance [5]. Increased fatty tissue requires more blood vessels to service it and adds to the total vessel length in the body [5].

2.2.9 Vessel Diameter

As shown in Equation 2.4, resistance varies inversely with the fourth power of the vessel radius (one-half the diameter, with the same volume). A smaller vessel diameter results in a greater amount of fluid to come into contact with the vessel's wall increasing resistance and pressure. Vessel diameter is actively regulated by vasomotor fibers**,** sympathetic nerve fibers that innervate the vessel's smooth muscle layer, causing constriction and dilation of blood vessels and in turn an increase or decrease in blood pressure respectively [5]. Norepinephrine, epinephrine, angiotensin II and vasopressin are chemicals which affect the blood vessel diameter (Figure 2.4) [5].

2.3 Blood Pressure Measurement Methods

As illustrated in Figure 2.5, there are two different types of methods for blood pressure monitoring: namely invasive and non-invasive methods [16]. The invasive method may be divided into two categories. The first is the catheter system, which is comprised of extra-vascular or intra-vascular pressure sensors, and the second concerns an implantable system, consisting of extra-arterial or intra-arterial sensors.

Although invasive techniques produce the most accurate results, the patient usually has to be hospitalized and a catheter is inserted into the artery which measures BP directly [16]. Therefore, non-invasive BPM is usually used instead for more routine monitoring. There are several methods for non-invasive blood pressure monitoring, such as auscultatory, oscillometry, palpation, ultrasonic, photoplethysmography, tonometry, pulse wave velocity, vascular unloading, and volume oscillometric [16]. Among these, the auscultatory and oscillometry methods are the most commonly used.

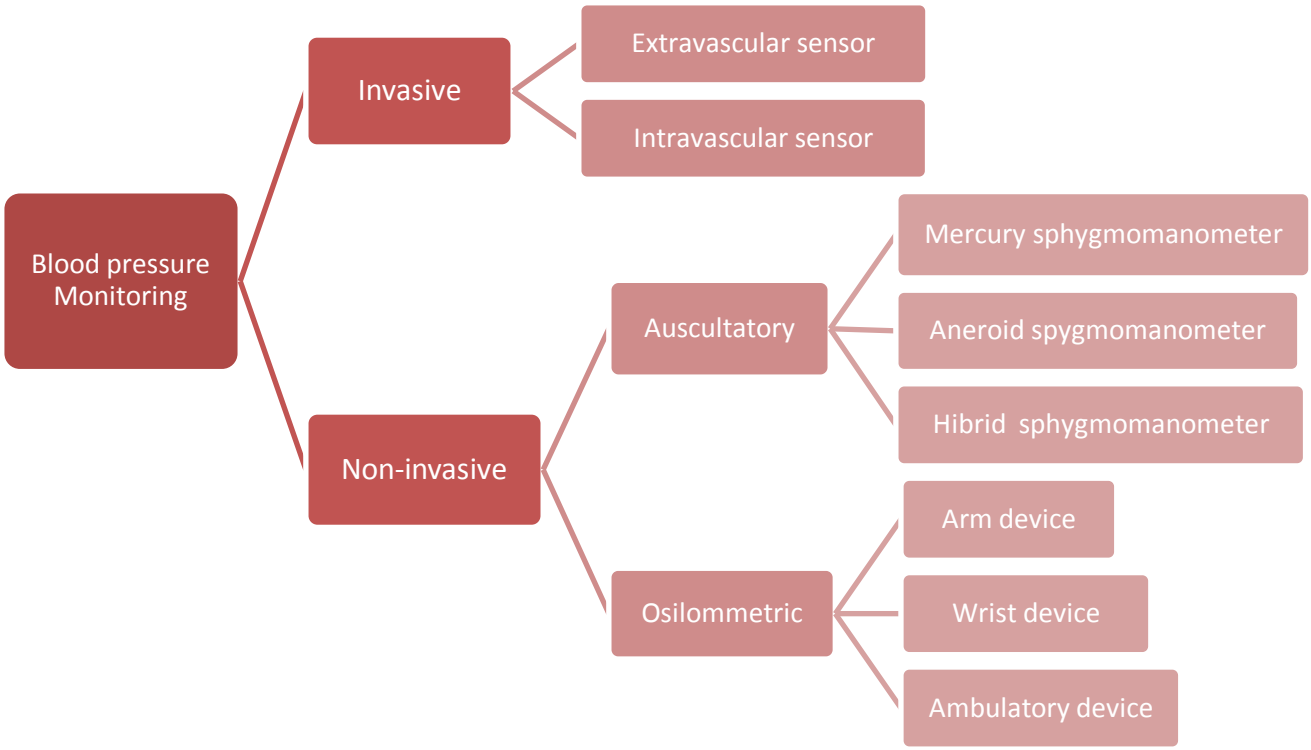

Figure 2.5 The methods used to measure blood pressure.

Technically, all devices for measuring BP are based on a gauge pressure sensor which leads to several problems. A gauge pressure sensor is a transducer which converts mechanical pressure into an electrical signal that is converted to a numerical value. The transducer can be located in the tip of a catheter for measuring BP invasively or incorporated into a cuff for detecting pressures associated with pressure turbulence or the oscillation of the walls of a vessel non-invasively. An electrical signal is the result of deformation of strain gauges which are attached to the diaphragm of the pressure transducer. In order then to measure BP, the gauge pressure sensor needs to be directly or indirectly connected to a pressure source (arterial vessel). It is important to note that this sensor requires frequent calibration to maintain the accuracy. Although most methods use gauge pressure to measure BP, it is not a true representation of the real pressure in

the arteries. Measuring gauge pressure is an indirect method to characterize the actual physiological forces that are due to the pumping of the heart. Consequently, current methods are often unreliable and must be frequently validated according to certain standards [17, 18] in order to maintain the accuracy [13]. Moreover, measurement accuracy depends on several significant factors which must be considered by physicians during the measurement such as posture and cuff size. Another problem with all available methods and devices is that each of them services a limited client base when measuring BP. For example, the oscillometric method, which is the most popular method used in automated devices, is not suitable for elderly and arrhythmia patients [6]. Currently, there is not one unique device that may be used for all patients with varying medical concerns, such as patients with hypertension or arrhythmia, elderly patients, pregnant women, and children.

2.4 Invasive Methods

With the invasive catheter method, the physician gains access to the artery by inserting a catheter inside it. Depending on the location of the pressure sensor, the catheter system can be divided into two types: extra-vascular or intra-vascular sensor system. In an extra-vascular sensor system, which is the most common clinical method, physicians connect the vascular pressure to an extra sensor element by using a liquid-filled catheter. On the other hand, in the intra-vascular pressure sensor, a pressure transducer is in the tip of the catheter and there is no need for liquid connection [10].

Although the invasive catheter method is considered the gold standard for blood pressure measurement, it is not routinely used because of several complications associated with it.

Consequently, it has been restricted to some surgical procedures, ICU monitoring, and some research applications. Complications with this method include the following:

1. Radial artery thrombosis: The catheter can cause artery thrombosis in up to 35% of the patients [19].
2. Pseudoaneurysm formation: Cannulation of the radial and dorsalis pedis arteries causes pseudoaneurysm formation more often compared to larger vessels [19].
3. Exsanguination: The unexpected disconnection of catheter tubing and pseudoaneurysm rupture may cause significant bleeding [19].
4. Peripheral nerve damage: This may occur from insertion direct trauma or by compression of the median nerve or brachial plexus by hematoma [19].
5. Distal artery vasoconstriction: It could minimize the measured BP leading to inappropriate use of vasopressors during shock [20].
6. Infection: Between 5 to 40% of patients experience infection at the insertion site as a result of sampling port contamination [20].
7. Increased cost: Invasive techniques are expensive as opposed to more affordable non-invasive counterparts. Because invasive methods require surgical cut-down or percutaneous insertion, the patient needs to be held under hospital care [10].

2.4.1 Extravascular Sensor Method

In this system, there is a hydraulic connection via the catheter between the source of pressure and the sensor element. The catheter, which is filled with a saline-heparin solution, must be flushed

with this solution every few minutes to prevent blood clotting at the tip. The following are common issues associated with this method [10]:

1. Blood clotting inside the vessel as a result of high temperature.
2. Electric (signal) drift as a result of tissue attachment or change of catheter position.
3. Fragility of the catheter.
4. Destructive sterilization is required.
5. Time delay and low frequency response as a result of the hydraulic connection between the pressure source and the sensor.

2.4.2 Intravascular Sensor Method

In this system, there is no hydraulic connection. The strain gauge has a flexible diaphragm which is used as a sensor at the tip of the catheter. Although it has fewer complications than extravascular sensor systems, the catheter may break after a few uses. This increases the cost per use making it more expensive than other BPM methods [10]

2.5 Non-invasive Methods

A typical system for a non-invasive BPM has a pressure transducer and an occlusive cuff which inflates to indirectly close the artery and then deflates. Pressure detection may be performed by a sphygmomanometer which can be mercury-based, aneroid-based, or use an electronic circuit in automated devices [10].

There are a number of techniques for non-invasive BPM such as auscultatory, oscillometry, ultrasonic, vascular unloading, and photoplethysmography. These methods have several shortcomings including:

1. They are less accurate than the invasive method [21]: The discrepancy between Korotkoff auscultatory measurements and intra-arterial readings may be as much as 25 mmHg [22].
2. They are not applicable for all patients: Non-invasive BP can be inaccurate among overweight and/or critically ill patients leading to erroneous interpretations of blood pressure [23].
3. They require frequent calibration: Each of the non-invasive devices, with the exception of mercury-based devices, need to be calibrated at least twice a year. Moreover, for calibrations, the devices need to be sent to the manufacturer. This procedure is not commonly performed in practice.
4. Incorrect cuff size is a major source of error [6, 7, 24-27]. An inflatable cuff bladder that is too narrow or too short will result in an incorrect BP reading [7]. Surveys have demonstrated that 96% of primary care physicians habitually use a cuff size that is smaller than it should be, and 25% do not even have a large cuff available.[13, 28], even though measurement errors tend to be smaller with larger cuffs [29].
5. Incorrect cuff placement [6, 13, 24-26]. It is necessary to place the cuff at the mid-point between the shoulder and elbow.
6. Inappropriate rates of cuff deflation contribute to error [24-26, 30].
7. Not able to measure BP continuously [31, 32].
8. Potentially lead to bruising: The use of cuff devices can cause petechiae and hematomas [33].

9. They are subject to the White Coat effect: All non-invasive BP devices can cause the White Coat effect, where the individual's BP increases artificially in the presence of clinical personnel.
10. Anxiety: Inflating the cuff causes increased tension on muscles that forces the closure of the artery. This is especially the case in patients suffering from hypertension, and more specifically, in an ambulatory setting whereby the BP device is attached to the person for 24 hours. It can also be uncomfortable when the subject is asleep as cuff inflation and deflation can interrupt sleep [34, 35].
11. Proper training for the caregiver or device monitor is required: It is necessary to have a trained individual using the device so as to obtain accurate BPM whether it is used clinically or at home [36].
12. There is typically a digit preference for numbers ending in a 5 or 0 [30].
13. With the exception of the mercury sphygmomanometer, there are differences in the accuracy of different brands [6]. Some devices available on the market do not pass accuracy protocol or validation standards [14, 37].

2.5.1 The Auscultatory Method

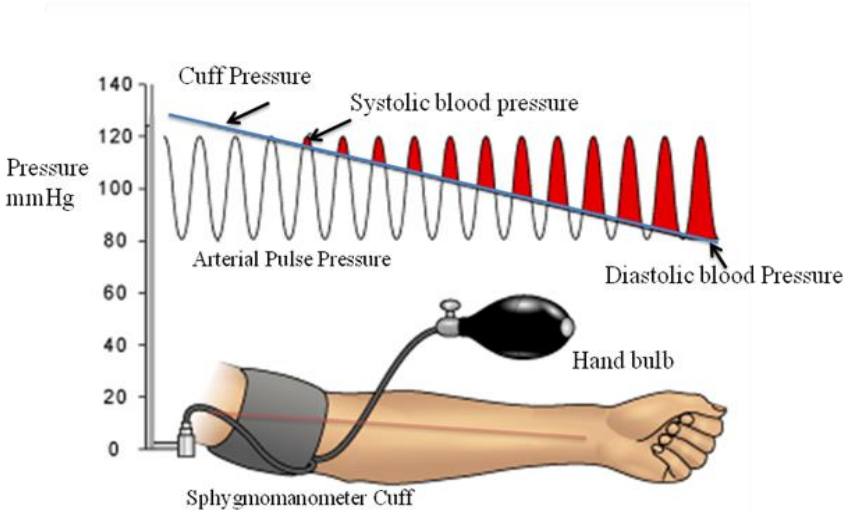

Figure 2.6 The Auscultatory Method (adapted from [12]).

Auscultation means listening for sound produced by the entire organ (i.e. vessels). The sounds are generated from a combination of turbulent blood flow and oscillations of the arterial wall, and are known as the Korotkoff sounds [5]. The auscultatory method relies on inflating an upper arm cuff to occlude the brachial artery and then listening to the Korotkoff sounds through a stethoscope whilst the cuff is slowly deflated (Figure 2.6). The patient's systolic and diastolic blood pressures are recorded from the readings on the sphygmomanometer at the start and end of the Korotkoff sounds, respectively [6, 10]. The auscultatory method can be read with mercury, aneroid, or hybrid sphygmomanometer [6]. The issues with this method include:

1. It is susceptible to observer error with the sphygmomanometer [6, 38].
2. It is inapplicable in a noisy environment [6, 7, 13].

3. It is difficult to hear the sound in some conditions (e.g. in older patients who have an auscultatory gap) [6], and is also not suitable for children under the age of five [7].
4. It underestimates systolic BP and overestimates diastolic BP [23], especially for obese patients [39, 40].

Mercury Sphygmomanometers

The mercury sphygmomanometer (Figure 2.7) is the ‘gold standard’ for non-invasive BPM. This includes a mercury manometer, an upper arm cuff, and a manual inflation bulb with a pressure control valve. It also requires the use of a stethoscope to listen to the Korotkoff sounds [8, 41].

Apart from the issues that are common with all auscultatory methods, the main issue with this device is that it contains mercury, which is toxic and so associated with disposal problems [6, 8, 25]

Figure 2.7 An example of Mercury Sphygmomanometer.

Aneroid Sphygmomanometers

Aneroid (i.e. without fluid) sphygmomanometers use mechanical parts to transmit the cuff pressure to a dial. The observer inflates and deflates the cuff manually while using the traditional auscultatory technique to identify systolic and diastolic pressures [14]. Aneroid Sphygmomanometers, as illustrated in Figure 2.8, are based on the same concept as mercury sphygmomanometer with an aneroid gauge replacing the mercury manometer.

Figure 2.8 An example of Aneroid Sphygmomanometer.

There are several complications involved with this device including:

1. Mechanical springs in aneroid do not provide stability over time. To maintain measurement accuracy, the device should therefore be regularly calibrated (at least every 6 months) [6, 7, 42].

2. It is susceptible to mechanical damage, especially when dropped [6].The frequency of defective devices in use can reach up to 35% [43-45].
3. It is less accurate than Mercury Sphygmomanometers [6, 42].
4. The accuracy of the manometers varies greatly from one manufacturer to another [6] with a range of inaccuracy from 1-44% [45-47].

Hybrid Sphygmomanometer

Hybrid devices combine both oscillometric (automated) and auscultatory (manual) features in a mercury-free device (Figure 2.9) [48]. The key feature is that the mercury column is replaced by an electronic pressure gauge similar to that in oscillometric devices. There are two types of hybrid sphygmomanometers. In the first, blood pressure is measured in the same way as mercury or aneroid devices. Applying the auscultatory method, the observer proceeds to use a stethoscope and listens to the Korotkoff sounds. The cuff pressure can be shown as a simulated mercury column, a digital readout, or as a simulated aneroid display. It can also be switched to the automatic oscillometric method. The second type consists of a button next to the deflation knob that is pressed at the operator's command at time points corresponding to the Korotkoff sounds, which then freezes the digital display to show systolic and diastolic pressures. This has the potential to minimize terminal digit preference, which is a major source of error with the auscultatory method. The hybrid sphygmomanometer has the potential to become a replacement of mercury because it combines some of the best features of both mercury and electronic devices.

Figure 2.9 An example of Hybrid Sphygmomanometer.

The disadvantages of these devices are as follows:

1. They are expensive [42]
2. They have not yet been fully validated.[4]
3. They underestimate BP, because of the delayed observer reaction and recognition time [6, 42, 48-50].

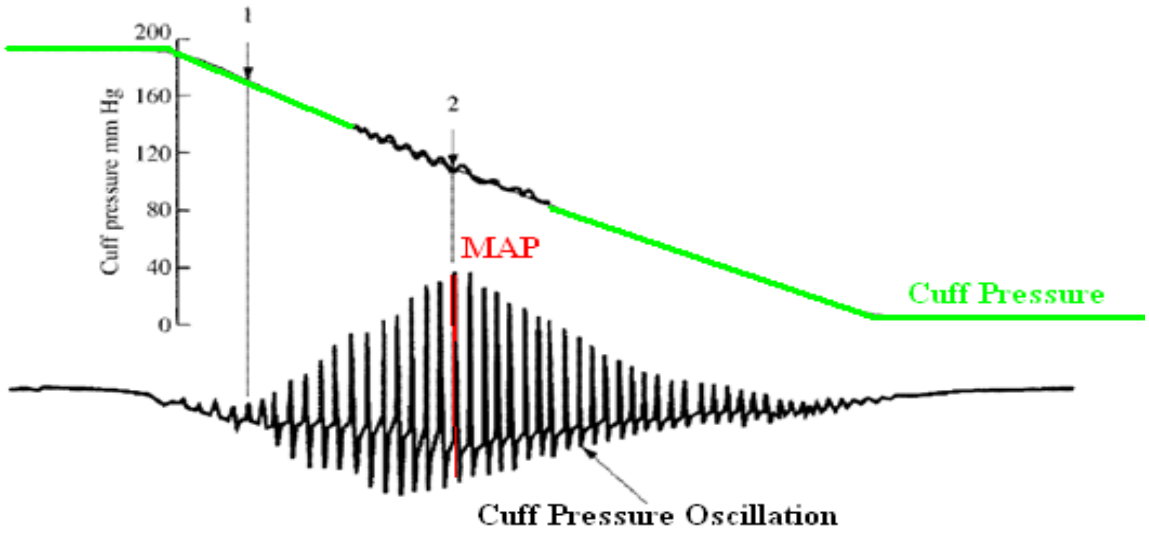

Figure 2.10 The Oscillometric Method (adapted from [16]).

2.5.2 The Oscillometric Technique

The oscillometric technique relies on automatic inflation and deflation of the device, with the cuff attached to a limb (usually the upper arm or the wrist). As demonstrated in Figure 2.10, a cuff is inflated above systolic pressure and slowly deflated. Systolic pressure is detected where there is a transition from small amplitude oscillation (Point1 in Figure 2.10) to increasing cuff-pressure amplitude. The cuff-pressure oscillations increase to a maximum (Point 2 in Figure 2.10) at the mean arterial pressure [16]. There is no clear transition in cuff-pressure oscillations to identify diastolic pressure since arterial wall expansion continues to occur below diastolic pressure. Thus, oscillometric monitors employ proprietary algorithms, that typically utilize so-called “characteristic ratios”, to derive the diastolic pressure – and sometimes systolic pressure – from the mean arterial pressure [16].

There are several issues involving this method, including the following:

1. The oscillometric method can accurately detect mean arterial pressure, but the estimation of systolic and diastolic is indirect and so is usually less accurate [51].
2. This technique is based on amplitude of the oscillation of the vessel wall which depends on various factors other than BP, specifically the stiffness of the arteries [6]. BP is significantly under-estimated in older people with stiff arteries and wide pulse pressures [52].
3. The algorithm for calculating systolic and diastolic pressures differs between devices and is not shared by the manufacturers.
4. There is a specific "bleed rate" according to each manufacture, which presumes a pulse between bleed steps in order to determine systolic and diastolic pressure [6].
5. Gender is an important factor in the accuracy in oscillometric method; oscillometric pressures accurately estimate diastolic BP in women, yet overestimate diastolic BP in men and underestimate systolic BP in both sexes [6].
6. This method is inaccurate in peripheral circulatory disorders, arrhythmias, [9, 23], diabetes, and many hypertensive /hypotensive patients.
7. There are many automated BPM devices that are readily available on the market, yet only a portion of them have been independently validated [17, 53].
8. This device is very sensitive to motion artifacts, and so cannot be used during physical activity [6].

Arm device

Arm devices (Figure 2.12) consist of an electronic monitor, pressure sensor, a digital display and an upper arm cuff [6]. The device automatically inflates, then deflates the cuff and determines the systolic and diastolic values, heart rate and/or pulse rate. This device may have built-in memory to record readings.

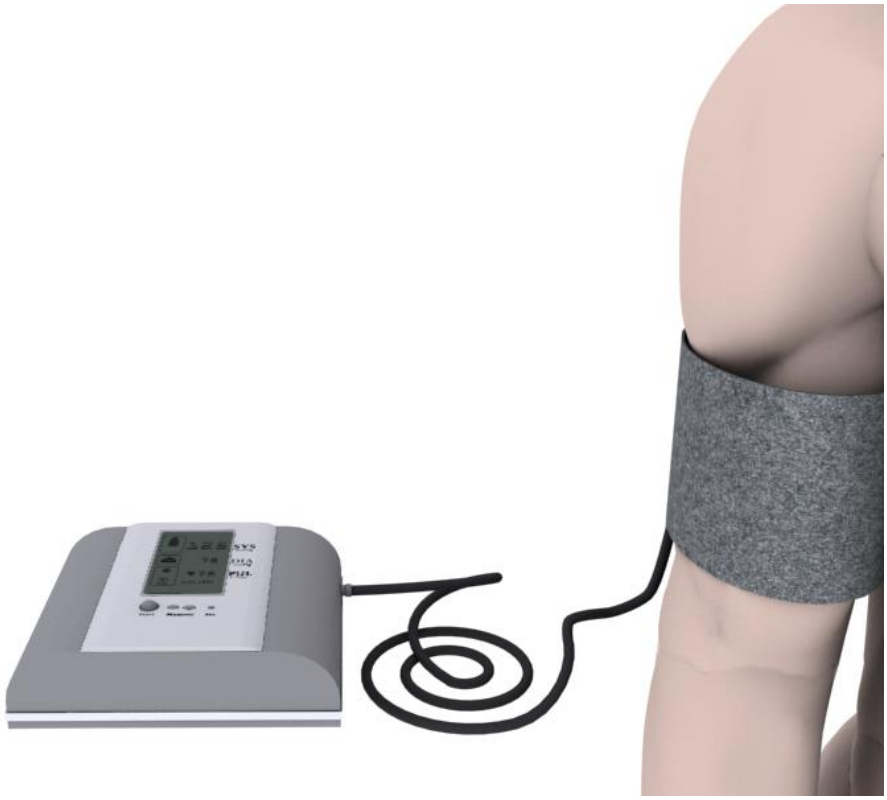

Figure 2.11 An example arm device.

Wrist device

A wrist device as shown in Figure 2.13, contains an electronic monitor, a pressure sensor, and an electrically driven pump attached to a wrist cuff [6]. The function is similar to the arm device. In comparison, the wrist device is smaller than arm device and its cuff is attached to the wrist. Its main disadvantage is that the wrist needs to be at the level of the heart to obtain an accurate measurement [6, 54].

Figure 2.12 An example of wrist device.

Ambulatory device

The Ambulatory BPM device is an arm device, but an electrically-driven pump is attached to the patient's belt [6] (Figure 2.14). To obtain a more comprehensive measurement of BP, the device

is attached to the patient for 24 hours. This device is based on auscultatory or oscillometric techniques. If based on the auscultatory method, it incorporates a microphone in the cuff and applies sound-based algorithms to calculate the systolic and diastolic blood pressure [6, 36, 41, 55].

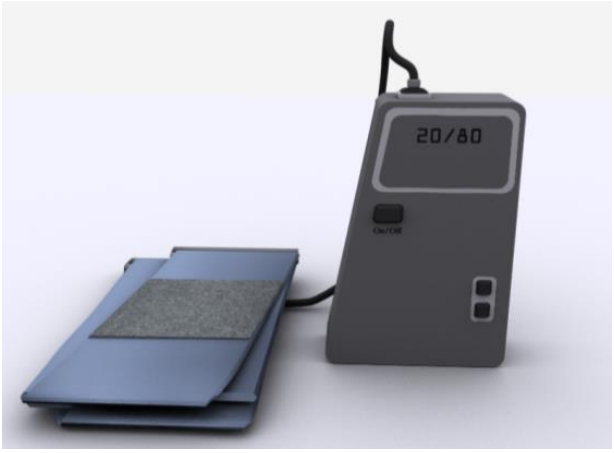

Figure 2.13 An example of ambulatory device.

The Ambulatory BPM device has the following disadvantages:

1. Cost: This device is the most expensive device in comparison with other non-invasive devices [22].
2. It has the same accuracy issues that affect other automated devices.
3. Current ambulatory BPM systems suffer from practical drawbacks. Users usually complain due to restriction in daily activities and mobility, noise, sleep disturbance, and pain. Therefore, such systems are not often not well-received by patients who use them [56, 57].

The following table summarizes the main issues associated with current methods for blood pressure monitoring.

Table 2.2 Issues with current methods and devices of blood pressure monitoring.

Method	Issues with method	Devices	Issues with device
Auscultatory	Susceptible to observer error [6, 38] Not applicable in noisy environments [6, 7, 13] Difficult to hear the sound in some conditions[6, 7] Requires a well-trained observer [6] Susceptible to stethoscope damage [7] Underestimates SBP and overestimates DBP [23] Inapplicable in obese patients[39, 40]	Mercury Sphyg.	Contains mercury, causes disposal problem [6]
		Aneroid Sphyg.	Susceptible to mechanical damage [6] Requires frequent calibration and service[6, 42] Less accurate than mercury [6, 42] • The accuracy of the manometers varies greatly from one manufacturer to another (Up to 44%) [6, 42]
		Hybrid Sphyg.	• Costly Still under

Oscillometric	• Very sensitive to motion artifact Not suitable for all patients (i.e arrhythmias, pre-eclampsia, diabetes, prepubertal children, and hypertensive /hypotensive and for the elderly) [6] • Difficult to calibrate • Individual calibration is needed Underestimates SBP and Overestimates DBP [23] • Originally designed for home use • Because of variety of algorithms for measurement, the accuracy of the method varies greatly from one manufacturer to another • Needs well trained observers • The bladders deflate at a manufacturer-specific "bleed rate," which assumes a regular pulse between bleed steps as part of the algorithms used to determine systolic and diastolic pressure		investigation[6] Underestimates BP [6]
		wrist	Less accurate than arm device [6] Should be at the heart level, during measurement [6]
		Ambulatory	Costly Not convenient [36] Restriction in everyday activities and mobility, noise, sleep disturbance, and pain [22, 56]

2.6 Cuffless blood pressure estimation methods

Two of the main disadvantages of conventional BPM devices are that they can be uncomfortable to use and they do not continuously provide estimates of blood pressure. Therefore the goal of developing cuffless devices is motivated by the fact that hypertension still remains poorly managed globally [58, 59]. Cuffless devices are still in the development stage and there are several research groups working since 2000 to design and implement a method/device to non-invasively and continuously measure blood pressure without cuff [59-64].

The most common cuffless BPM methods are based on 3 main related parameters; the measurement of pulse wave velocity (PWV), pulse transit time (PTT), and pulse arrival time (PAT). The pulse arrival time (PAT) defins as the time-delay between the R-peak of the QRS complex from the ECG and the arrival of the arterial pulse wave at a peripheral point in the arterial system [59, 60, 62 and 63]. As shown in Figure 2.15, the PAT is the summation of the pre-ejection period (PEP) with the pulse transit time (PTT).

$$PAT = PEP + PTT \qquad (2.5)$$

PAT and PTT are typically measured with the Electrocardiogram (ECG) and photoplethysmography (PPG). The PEP is the duration of the iso-volumetric ventricle contraction up to the aortic valve opening and is a non-constant additive delay, which changes rapidly in response to stress, emotion and physical effort [60-63]. The PTT is measured as the time interval from the R-peak to a characteristic point at a predetermined threshold on the photoplethysmographic (PPG) pulse of the same cardiac cycle [60]. The PTT is the true transit time of the pulse along the arterial wall over a long non-homogeneous vascular path.

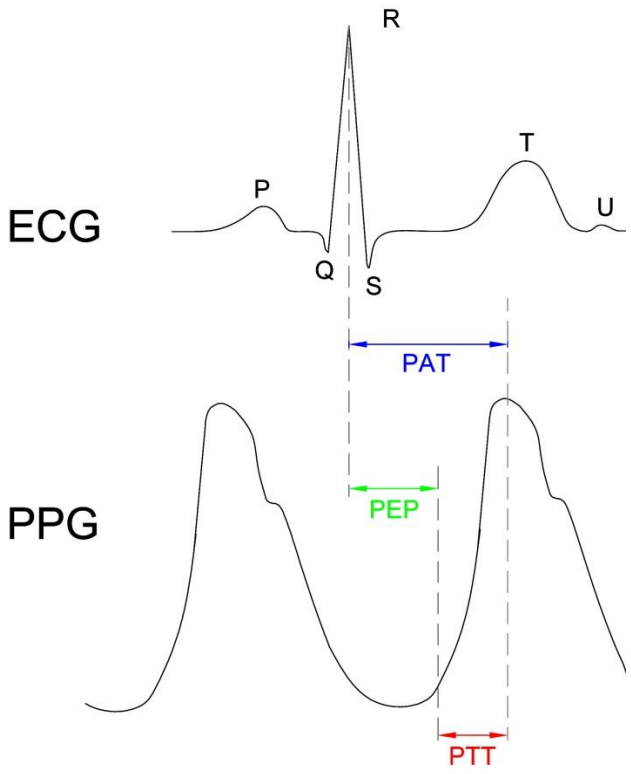

Figure 2.14 Pulse Arrival Time (PAT); PAT=PTT+PEP.

The PWV can be calculated based on the Moens-Korteweg equation and depends on vessel wall elasticity as in the following equation [11]:

$$\text{PWV}=\frac{Distance}{PTT}=\sqrt{\frac{Eh}{\rho 2r}} \qquad (2.6)$$

where ρ is the blood density, r the vessel radius, h the wall thickness and E the Young`s elasticity modulus of the wall [64]. It is assumed that ρ, r and h have small changes, with the main variations coming from the elasticity [65]:

$$E = E_0 e^{\alpha P} \quad (2.7)$$

where E is the elasticity, α is a constant number typically taken as 0.017 mmHg, and P is blood pressure. The combination of Young`s module and the Moens-Korteweg equation leads to the following form [66]:

$$SBP = A(L/PAT) + B \quad (2.8)$$

where A is a constant sensitivity factor which is the averaged over all subjects, the parameter B is individually adapted for each person and, and L is a subject‘s arm length.

A constant parameter A is usually used for healthy subjects whereas B must be tuned to each subject based on SBP and PAT measurements done at rest (Figure 2.16).

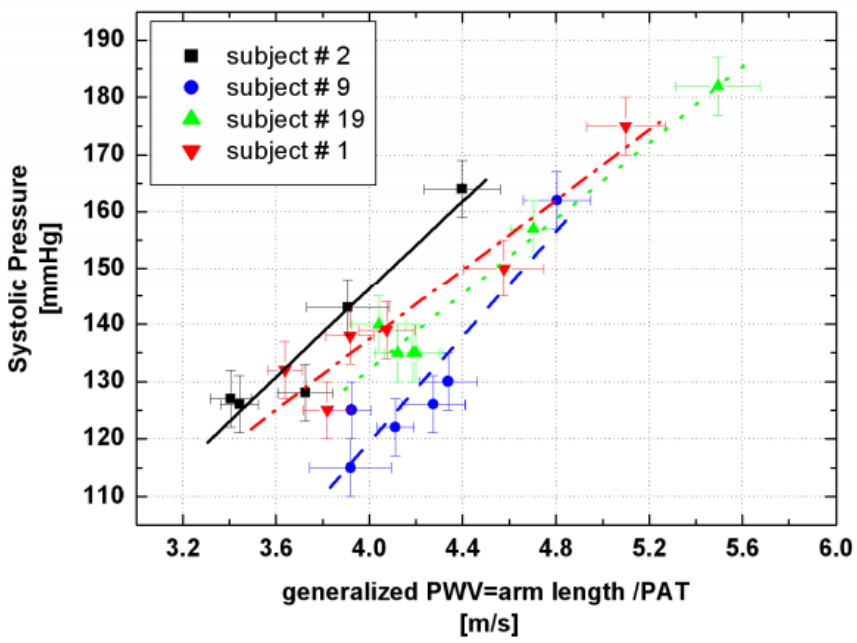

Figure 2.15 SBP vs. generalized PWV that is defined by the ratio of a subject's arm length over PAT (adapted from [62]).

2.6.1 Applications

These cuffless methods have been applied in different devices such as wireless and wearable Body Sensor Networks (BSN), in personal digital assistants (PDA), or in a wristwatch and have been used to transfer the data to health care centers for 24/7 continuous monitoring of blood pressure [59-63, 67-69].

2.6.2 Limitations

A main problem with this technique is that it cannot measure or estimate diastolic BP. Therefore, it is not realistic for clinical use especially for hypertension patients who have high diastolic pressure [61-63, 69]. There are also accuracy problems with this method as it does not achieve the requirements of standards protocols such as ANSI/AAMI for SBP [59, 60, 67].

Another limitation of this method is that it makes many assumptions that may not be correct and so contribute to the inaccuracy. For example, the method assumes that the PEP is constant which is not correct. Muehlsteff et al., 2006 shows that an accurate value of PEP is important especially during physical activity and can substantially change the estimate of SBP [62]. Additionally the parameters ρ, r and h are also different in different individuals. For this reason, individual calibration is also needed, but this requires developing an appropriate method for calibration, which is not available yet. Furthermore, this method is not always convenient because it requires wearing ECG leads that are attached to the chest of the person, which can be uncomfortable for long term monitoring. Therefore given all these difficulties, there is still the lack of a device

which is light, easy to use, comfortable, that is able to measure SBP and DBP continuously and accurately without a cuff and that does not need of individual calibration.

2.6.3 Machine Learning Approach

Figure 2.4 shows some of the internal physiological factors that affect BP. However, there are many other physical and non-physical factors (e.g., emotional state, posture) that affect the blood pressure level over a very short duration (even within a few heartbeats). Therefore, it is very difficult to develop a mathematical equation which includes all relevant factors to calculate accurate BP values. As a result, a possible solution to overcome this limitation is artificial intelligence and machine learning instead of using an algebraic formula. Some researchers are trying to use different machine learning algorithms with the pulse wave signal of the PPG that can be obtained easily and non-invasively to estimate blood pressure continuously.

Suzuki et al. in 2009 used PPG to get Pulse Wave (PW) signal to estimate SBP by Error-Correcting Output Coding (ECOC) method as a multi-classifier machine based on an aggregation of general binary classifiers. However, in the end, this method could not achieve a standard deviation of error values less than 8 mmHg, as required by the ANSI/AAMI standard [70].

Aboui et al. in 2011 used an Artificial Neural Network (ANN) with two parameters of blood concentration and heart rate to predict the MAP for hemodialysis patients [71]. They reported an error of 9%, but their study was restricted to MAP and did not estimate SBP and DBP [61].

Monte-Moreno in 2011 used several machine learning algorithms such as linear regression, neural networks, support vector machines, and random forest to estimate BP from PPG signals.

To select the best structure and parameters, they used 70% of the database as training and 10% for validation and 20% for testing. This was done 10 times by rotating the databases. They collected data from 213 male and 197 female volunteers (410 in total), aged from 9 to 80 years (mean±SD=37.97±13.32). Each subject's PPG was measured with the fingertip pulse oximeter device iPod Digital Oximeter and BP measurements were made an aneroid sphygmomanometer. The input of the signal was PPG signal and the outputs are SBP and DBP. [72], and the following is a description of each of the methods used:

• Linear regression (LR). For the linear regression method, they trained a univariate model $y^j = \beta_0^j + \sum_{i=1}^{n} \beta_i^j X_F(i),$ where j= {SBP and DBP} using the ridge regression algorithm. The quality criterion was the coefficient of determination R2 value on the test set.

• Neural networks (NN). For the neural networks method they used a multilayer perceptron trained by means of a conjugate gradient algorithm (Fletcher Powell). They used 1 hidden layer with 10 nodes, and three at the output, and a hyperbolic tangent algorithm. The quality criterion was the coefficient of determination R2 value on the test set.

• Support vector machines (SVM). For SVM regression, they used the ε-insensitive loss function and the kernels were the Gaussian and the polynomial and standardized the data. The values of sigma were varied from 0.1 to 5, and for the polynomial kernel, orders from 1 to 5 were tested. The best kernel was a Gaussian kernel. The quality criterion was the coefficient of determination R2 value on the test set.

• Random forest (RF). The performance of the RF was insensitive to variations of the parameters in a certain margin, i.e., for a number of trees higher than 30 there was no improvement, and the size of the set at each node could vary from 1 to 10 without worsening

the performance. The RF has a method for ranking the features based on how the performance degrades when a given input feature is randomly permuted in the test.

In conclusion, their system complies with Grade B of the British Hypertension Society's protocol, which is considered the minimum to pass the accepted criteria of the International Protocol or the AAMI Protocol.

Kurylyak et al. in 2013 also used an ANN method with the PPG signal to estimate BP. They extracted features from the PPG signal and employed a Kalman filter for preprocessing their data [73, 74] . Chapter 3 Section 3.7 describes in detail how they extracted their features from the PPG signal. They took 5000 separate PPG signals in individual heartbeats for different persons and different time instances from the same online source that we used (MIMIC II database at physionet.org) and these were identified with corresponding BP values using the invasive arterial BP (ABP) signal to obtain the reference values for comparison with their estimated values [77 , 82]. Then 21 parameters were extracted from each of the separate pulses, and these parameters defined the input vector for the ANN. A multilayer feed-forward back-propagation ANN architecture with two hidden layers was used, with 35 neurons in the first hidden layer and 20 in the second one and two output neurons to simultaneously estimate SBP and DBP. The performance results of their experiments on the test database presented as mean and standard deviation of absolute error (MAE±SDAE) obtained from reference SBP/DBP and estimated values. In their tests, the error in for of MAE±SDAE is 3.80±3.46 mmHg for systolic and 2.21±2.09 mmHg for diastolic pressure which fulfil the requirement of common standards. They used a Kalman filter to remove the low and high frequency noise (by eliminating artifacts from the reference signals used to train the ANN) and as such obtained an increase in the accuracy of estimated BP. The error for SBD and DBP with Kalman filtering became 3.24±3.47 and

1.79±2.02 respectively and the improvement with respect to unprocessed date was about 20% [77, 82]. They, however, did not describe how many subjects were included in their 5000 pulse dataset To train their network, they used 70% of collected heartbeats, and used 15% for validation and 15% for testing. It is not clear, however, if they separated the subjects into each of these subsets or if they allowed pulses from an individual subject to be represented in the training, validation, and testing sets. Additionally, although they report meeting the requirements of the ANSI/AAMI standard, they evaluate the performance of their method in the form of mean absolute error (MAE) and standard deviation of absolute error (SDAE) and not mean error (ME) and standard deviation of the error (SDE), as required by the standard. In our work, we also consider the ANN as a solution to estimate BP from the arterial pulse waveform, as described in the next chapter.

3 Materials and Methods

3.1 Introduction

The analysis approach used to estimate BP pressure from the arterial pulse waveform is based on an Artificial Neural Network (ANN). An ANN consists of an input layer, one or more hidden layers, and an output layer [73]. Figure 3.1 shows an example of an ANN with an input layer, one hidden layer with 3 neurons and one output layer with two neurons. Each layer could consist of one or several nodes which are called neurons. Similar to a typical natural neural network, the ANN connections run forward from input to hidden nodes and from hidden nodes to output nodes, which is why it is called Feed-forward. However, during the training phase, the system could have a feedback loop that takes the errors from the output back to hidden nodes causing the weights on connections to change. This is called backpropagation, and can increase the accuracy of the system [73]. The process of implementing an ANN has 3 steps; training, validation, and testing. In the training step, the program is presented with example inputs, desired outputs, and tries to learn to map inputs to outputs. In the validation step, the system validates the results from training and optimizes the network structure. In testing, the algorithm is given a new input and is asked for an estimated output based on the network built in the previous steps. In the end, the performance of the network is evaluated by calculating the error based on a comparison between reference and estimated values. [73-75]

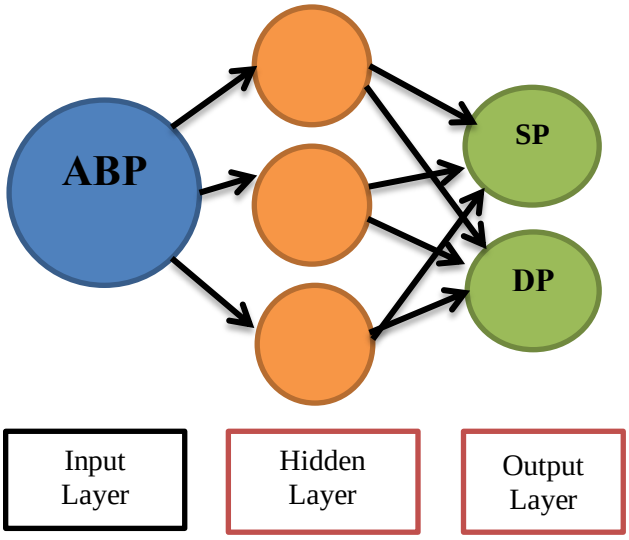

Figure 3.1 An example of ANN with the input layer, one hidden layer with 3 neurons, and one output layer with two neurons. ABP is arterial blood pressure, SP and DP are systolic and diastolic pressure, respectively.

In this thesis, the ANN is chosen as a solution for BP estimation because it is a powerful tool for nonlinear modeling. The main advantages of ANN are: 1) It can learn a complex nonlinear relationship with limited prior knowledge, and 2) It can perform inferences for an unknown combination of input variables [73-75].

Figure 3.2 illustrates a block diagram representation of the proposed algorithm for BP estimation that is based on an artificial neural network:

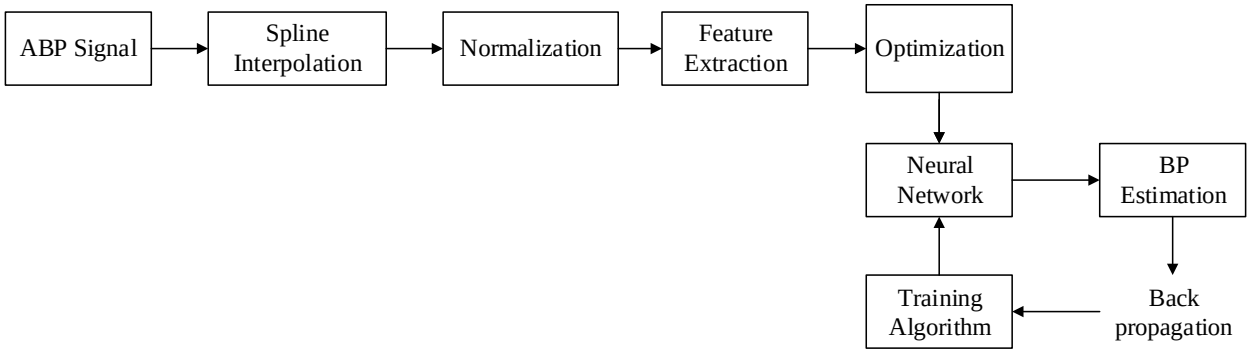

Figure 3.2 A block diagram of the proposed ANN method.

3.2 Arterial Blood Pressure (ABP) signal

The invasive arterial blood pressure (ABP) signal is used as input to the ANN. However, as a first step, it is normalized to a value between 0 and 100 to avoid providing the network with calibrated pressure information. That is, the only information made available to the network is the uncalibrated waveform shape. On the other hand, to evaluate the performance of the ANN, the peaks and troughs of the ABP signal, prior to normalization, are used as calibrated reference values of systolic and diastolic blood pressures, respectively.

The ABP signals are obtained from the MIMIC II (Multi-parameter Intelligent Monitoring in Intensive Care) database available through the physionet.org website. This online database contains physiological signals and vital sign time series captured from patient monitors obtained from intensive care unit (ICU) patients.

Based on the ANSI/AAMI standard, there are two methods allowed to evaluate the accuracy of a new method for measuring BP: The intra-arterial method or auscultatory method [76]. If the intra-arterial method is used as the reference, no fewer than 15 subjects should be used with 10

paired measurements per subject, for a total of 150 paired observations. If auscultatory method is used as the reference, there should be no fewer than 85 subjects with 3 paired observations each, for a total minimum of 255 (= 3*85) paired observations. For SBP and DBP separately, the mean error (ME) of the 255 individual paired measurements of the test system should be ± 5 mmHg or less, with a standard deviation of error (SDE) of 8 mmHg or less. In this research, the intra-arterial method is used as the reference measurement because accurate calibrated values of SBP and DBP are readily obtainable from the ABP signals. Therefore, from the MIMIC II database, the ABP signal from 11 ICU patients with normal blood pressure and 11 ICU patients with hypertension are used with 10 periods each, for a total of 220 paired ABP signals as inputs to train and test the ANN. At the very end, to test the performance of the ANN with a completely "fresh" set of data, a further 2 patients with normal blood pressure and 1 patient with hypertension with 10 periods each are used. Figure 3.3 shows the distribution of systolic and diastolic pressures of the aforementioned 22 patients. Note that a single cardiac pulse period of the ABP signal is considered as one input waveform to the ANN.

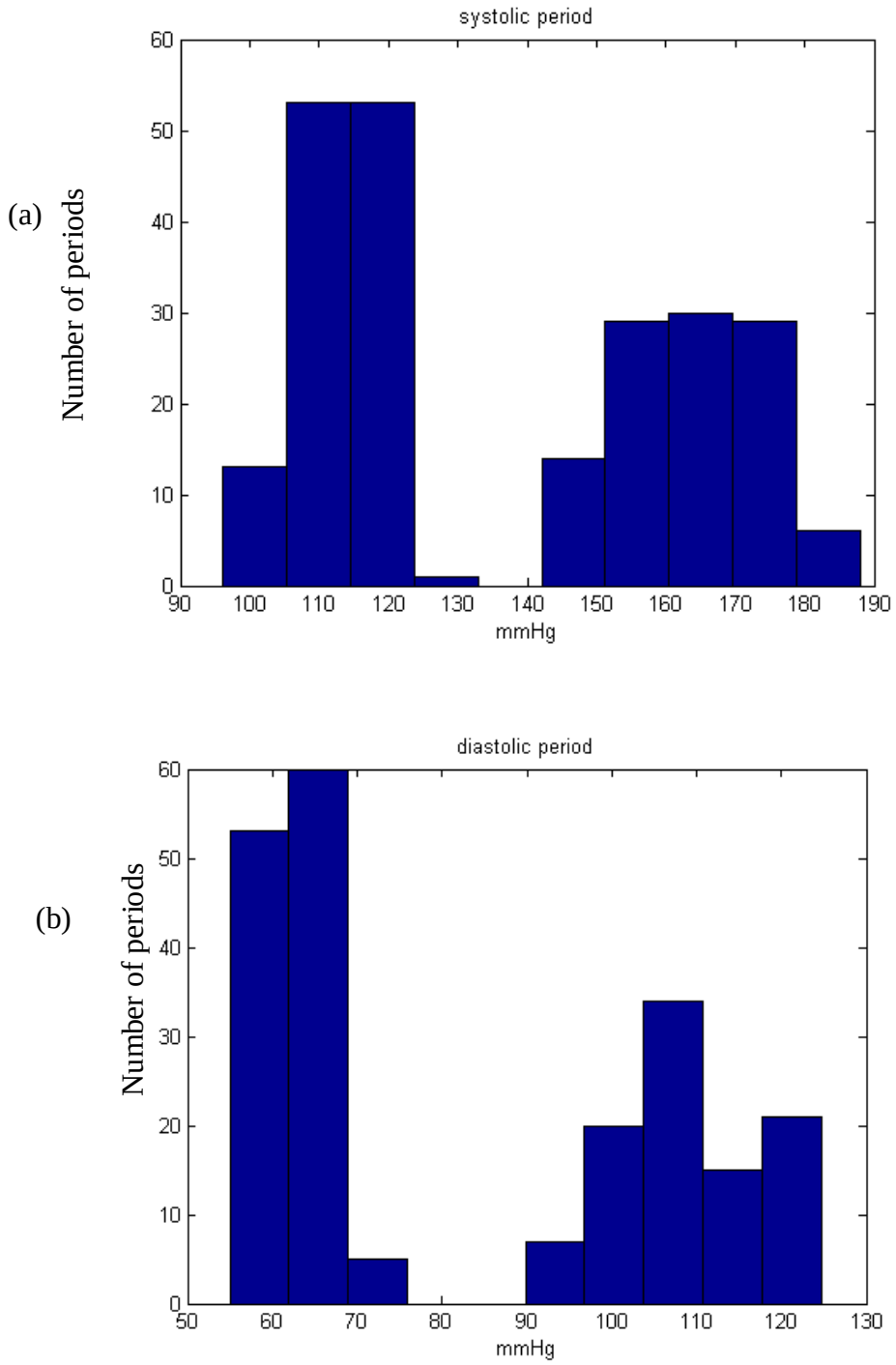

Figure 3.3 The histogram of (a) systolic and (b) diastolic distribution for the 22 ICU patients used to train and test the proposed ANN.

Figure 3.4 (a) shows an example of a one minute recording of the ABP signal for a patient with normal blood pressure. The first 10 periods of this signal are selected as the input of the ANN (Figure 3.4 (b)). Figure 3.4 (c) illustrates a complete period which could be from minimum to minimum for estimation of the SBP and peak to peak for estimation of the DBP (the reason for using these two different start and end points for the SBP and DBP is explained below). The reference systolic and diastolic BP are calculated as the maximum and minimum of these signals within the cardiac pulse.

(a)

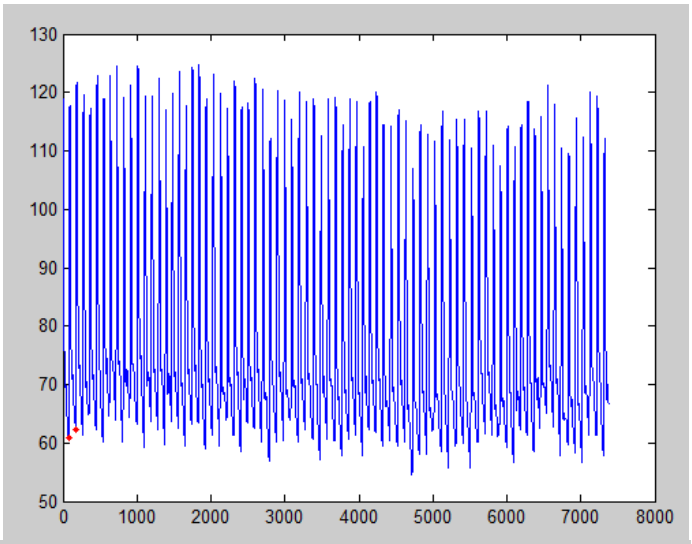

(b)

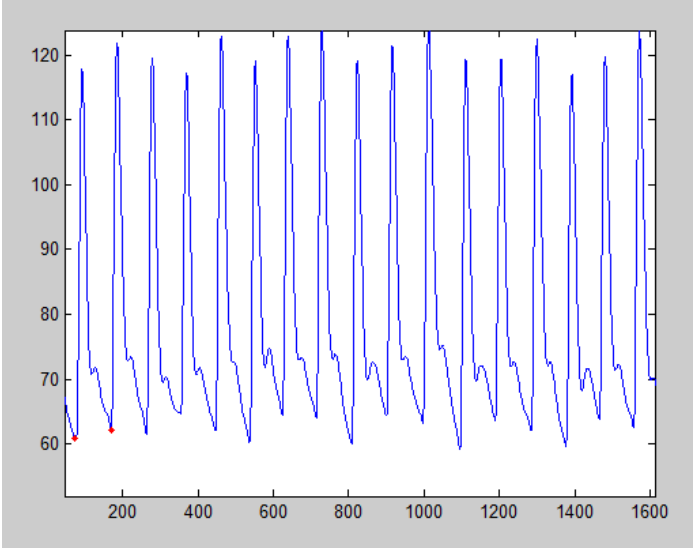

(c)

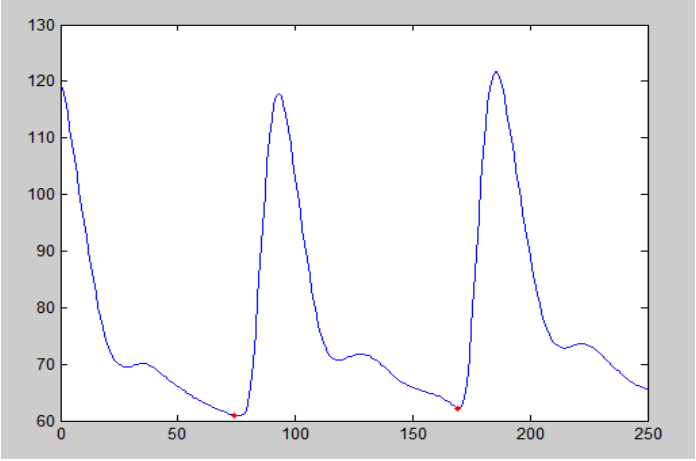

Figure 3.4 An example of an ABP signal for one patient. (a) One minute recording. (b) The selected 10 periods. (c) One minimum to minimum selected period.

3.3 Spline Interpolation

In each person, the amplitude and duration of the pulse signal varies beat to beat which means that each single period consists of a different number of samples. However, since the number of input neurons in the ANN must be fixed when the raw signal is used as input to the network, all pulse periods are interpolated to 100 samples (x-axis in Fig. 3.5), making the input matrix to the network a 220 periods x 100 samples. Figure 3.5 shows an example of (a) the original ABP and (b) the interpolated signal.

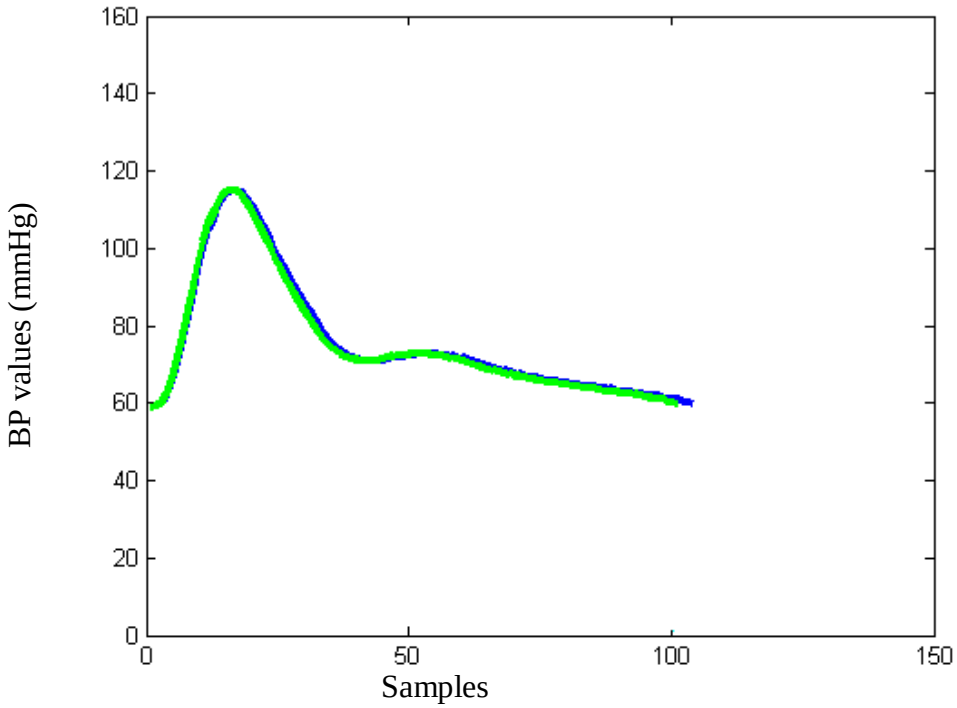

Figure 3.5 An example of ABP signal: the raw signal is in blue and the interpolated signal is in green.

3.4 Normalization

The ABP signal in each pulse period used as input to the ANN is normalized from 0 to 100 to make sure that the network is not provided with calibrated information about the blood pressure, and so it only uses the shape of the signal to estimate the SBP and DBP. Normalization also helps the ANNs train faster and reduces the chances of getting stuck in local minima [121]. Figure 3.6 illustrates an example of (a) the original ABP after interpolation (Section 3.3) and (b) the normalized signal.

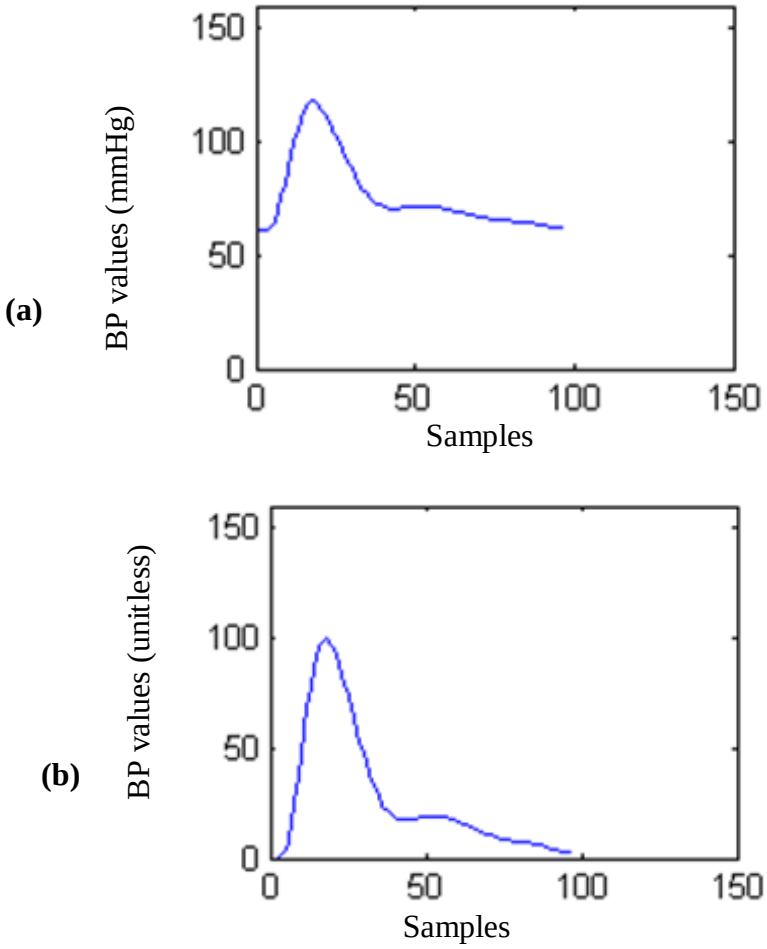

Figure 3.6 An example of ABP signal. (a) The raw signal after interpolation. (b) The normalized signal.

3.5 Artificial Neural Network (ANN) architecture

Because the proposed method is intended in the future to be implemented in a stand-alone cuffless BPM device, the required size of memory is one of the considerations of this research study. Therefore, a multilayer feed-forward (FF) architecture that uses backpropagation for training is proposed and not another ANN architecture based on the radial basis function, counter propagation, or learning vector quantization, because this architecture requires a smaller number of neurons in the case of large training set [77].

The Levenberg-Marquardt backpropagation algorithm (trainlm function in MATLAB) is a network training function that updates weight and bias values. The reason that this training function is chosen is because it is often found to be the fastest backpropagation supervised algorithm. It has gradient descent and adaptive learning and back propagation all included it, and therefore it is a good choice for optimization of the network [74].

Although the network uses a fixed training function (Levenberg-Marquardt) and, once optimized, a fixed number of hidden layers and neurons, it has a random weight and bias each time when the network is run. Therefore, based on the central limit theorem in statistics, to get a good estimate, the program is run 30 times, with 30 times in training, validation and testing. At the end, the average values of errors, in the testing phase, are calculated based on these runs in the form of mean error (ME) and standard deviation of error (SDE) (as shown in Table 4.1).

The leave-one-out method is used for testing the ANN. In this method, one patient and all his/her 10 associated periods are removed from the 220 waveform dataset to avoid biasing the training of the network and used for testing. Therefore, 210 waveforms remain for training and validation of which 80% (168 waveforms) are used for training and 20% (42 waveforms) are used for the

validation. The ANN model is designed using MATLAB R2012a (The MathWorks, Natick, Massachusetts).

3.6 Principal component analysis (PCA)

The input to the ANN has 100 samples per waveform and so has high dimensionality. Therefore, a dimensional reduction process is applied on the signals based on linear time series analysis. Principal Component Analysis (PCA) is a dimension-reduction approach that can be used to reduce a large set of variables to a small set that still includes most of the information found in a large set. A subset of variables from a larger set is selected, based on which original variables have the highest correlations with the principal component [73]. PCA is commonly used for this purpose and has been found to show satisfactory results in many applications where dimensionality reduction is needed [73].

Based on our experimental design in this thesis, PCA is applied on the raw signal and also on the 21 features that are extracted from the pulse signal (Section 3.7 below). In the end, the results with and without dimensionality reduction are compared to see whether or not using PCA improves the results.

3.7 Feature Extraction

Our goal is to estimate the systolic and diastolic blood pressure from the pulse signal. This goal could be approached by a non-invasive device that measures the pulse signal using an optical sensor such as in a pulse oximeter or which could be embedded in a smartphone. The amplitude

of the obtained pulse signal may change due to several factors such as the gain of the device, the amount of the pressure between the finger and the optical sensor etc. As a result, the amplitude of the signal would not contain useful information for estimating the blood pressure. Therefore one approach would be to characterize the pulses considering features that reflect the temporal structure of the signals.

Several parameters could be used in order to characterize the ABP pulses. The following are the parameters obtained based on a review of the literature: The Systolic Upstroke Time (SUT), Diastolic Time (DT), time width of 2/3 and 1/2 pulse amplitude, are mentioned in [78], while the cardiac period (CP) and peak width at 10% of the pulse height are used in [79]. Kurylyak et al. (2013a) also proposed to calculate the width at 25%, 33% and 75% of the pulse height and to extract separate features for the systolic and diastolic components which are the intervals from minimal to the maximal point and from the maximal to the next minimal point, respectively [77]. These authors also proposed using the ratio between systolic and diastolic widths (DW/SW) as well as their sum in order to extract as much information as possible (SW+DW), for each of the 10, 25, 33, 50, 66 and 75% time periods (x-axis). Thus, they extracted 21 parameters as a feature set for the pulse signal as follows (Figure 3.7):

- Cardiac Period (CP), Systolic Upstroke Time (SUT), Diastolic Time (DT);
- At 10%: DW10, SW10+DW10, DW10/SW10;
- At 25%: DW25, SW25+DW25, DW25/SW25;
- At 33%: DW33, SW33+DW33, DW33/SW33;
- At 50%: DW50, SW50+DW50, DW50/SW50;
- At 66%: DW66, SW66+DW66, DW66/SW66;
- At 75%: DW75, SW75+DW75, DW75/SW75

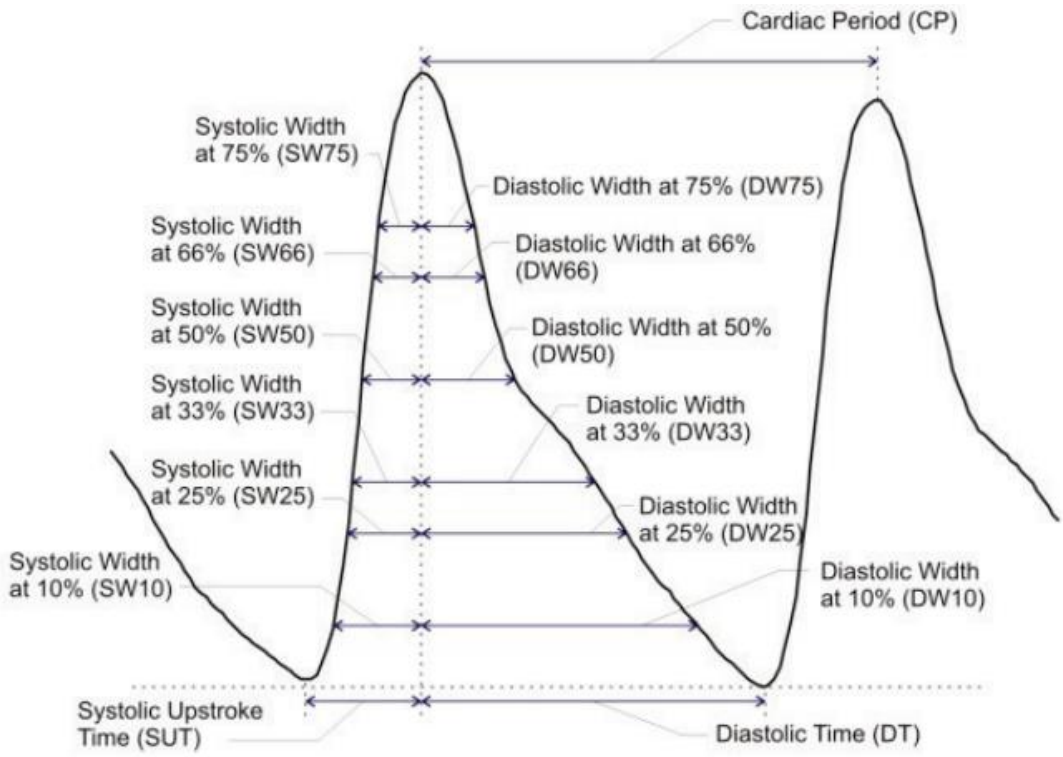

Figure 3.7 The 21-features extracted from the ABP signal (adapted from [77]).

3.8 Analysis Procedures

The following four sets of features are used as inputs to the ANN and the obtained results are compared:

Input 1: Raw Signal

Input 2: PCA of the Raw Signal

Input 3: 21 Extracted Features (described in Section 3.7)

Input 4: PCA of 21 Extracted Features

In all procedures, to increase the accuracy of the result, separate networks are used for systolic and diastolic blood pressure estimation. With 220 input pulse periods in total, the ANN estimates 220 SBP and 220 DBP values.

3.8.1 Procedure 1: Raw Signal as input

As illustrated in Figure 3.8, in this procedure, the input feature set consists of 100 sample values for each period. Then the signal is interpolated and normalized as described in Sections 3.3 and 3.4 before using it as input to the network that is optimized. The optimized network (Section 3.9, Table 3.1) for SBP consists of 3 hidden layers with 8, 7, and 6 neurons, respectively. The optimized network for DBP consists of 2 hidden layers with 5, and 6 neurons respectively.

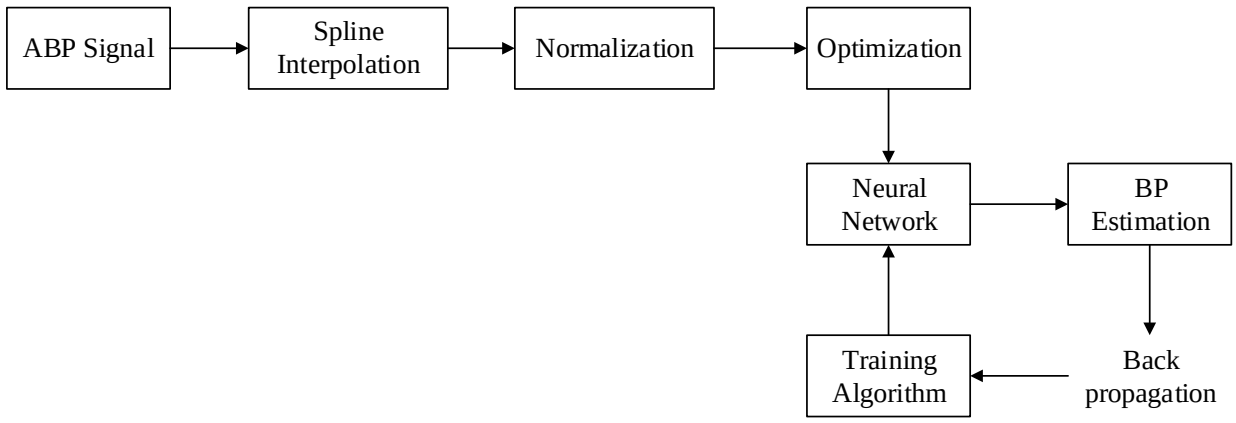

Figure 3.8 The block diagram of Procedure 1, with the raw signal as input.

3.8.2 Procedure 2: PCA of the Raw Signal as input

In this procedure, after interpolation and normalization of the ABP signal, Principal Component Analysis (PCA) is applied on the raw signal for each input pulse period (Figure 3.9). The output of the PCA is used as input to the ANN, giving a feature set with 6 elements for SBP and a feature set with 4 elements for DBP. These numbers of PCA elements for systolic and diastolic pressure covered 99% of the information in the raw input signal.

As shown in Table 3.1, the optimized network for SBP consists of 1 hidden layer with 2 neurons. The optimized network for DBP consists of 2 hidden layers with 8 and 7 neurons, respectively.

The PCA is applied only in training phase of the procedure, and the validation and testing phases used the PCA which was determined in the training phase.

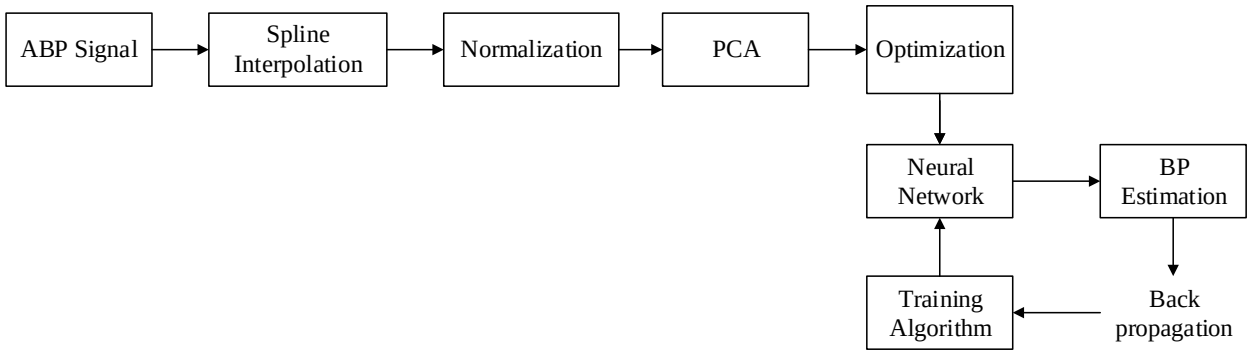

Figure 3.9 The block diagram of Procedure 2 with the PCA of the raw signal as input.

3.8.3 Procedure 3: 21 Extracted Features as input

In the third procedure, the 21 features extracted from each raw pulse signal, as described in Section 3.7, were used as the input feature set (Figure 3.10). As indicated in Table 3.1, the

optimized network for SBP consists of 2 hidden layers with 10 and 20 neurons, respectively. The optimized network for DBP consists of 2 hidden layers with 3 and 2 neurons, respectively.

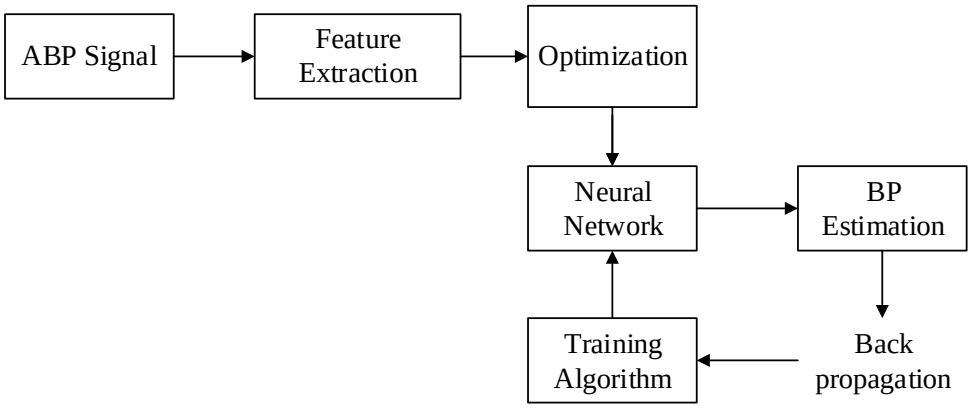

Figure 3.10 The block diagram of Procedure 3, with 21 Extracted Feature as input.

3.8.4 Procedure 4: PCA of 21 Extracted Features as input

The fourth procedure is the same as Procedure 3 except that PCA was applied to the set of 21 extracted features (Figure 3.11), giving a feature set of 6 elements for the SBP and a feature set of 4 elements for the DBP. These numbers of PCA elements for systolic and diastolic pressure covered 99% of the information in the raw input signal. The optimized network for SBP consists of 1 hidden layer with 2 neurons. The optimized network for DBP network consists of 2 hidden layers with 8 and 7 neurons, respectively (Table 3.1).

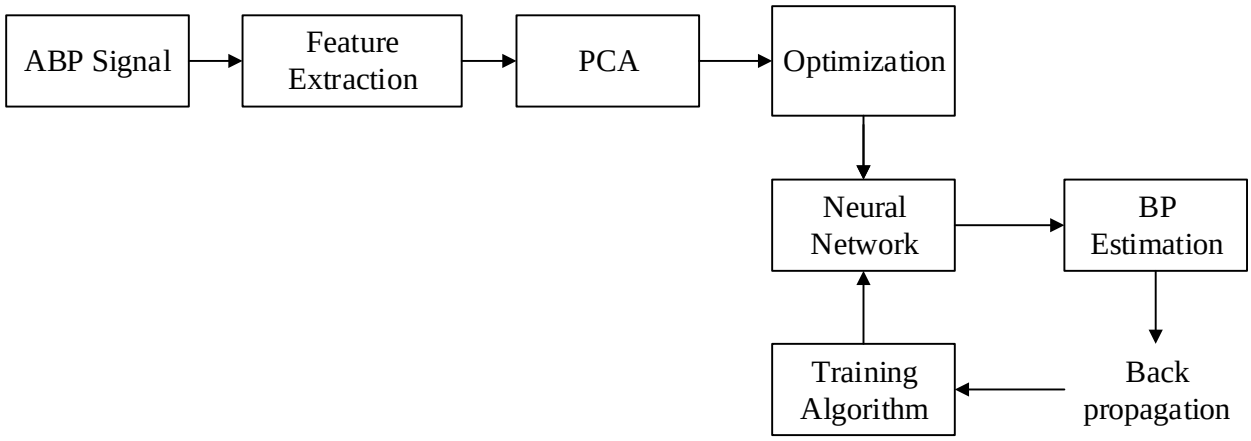

Figure 3.11 The block diagram of Procedure 4, with PCA of 21 Extracted Features as input.

3.9 Optimization

An important part of implementing an ANN to estimate SBP and DBP is optimizing the network structure. The most popular approach for finding the optimal number of hidden layers and neurons in each layer is by trial and error. In our approach, we designed the networks for systolic and diastolic pressures separately and found the optimized structures for them separately. For SBP, the boundaries of the pulse were either peak to peak or minimum to minimum (min to min), and similarly for DBP the boundaries of the pulse were either peak to peak or min to min. With trial and error, to find the best structure for the number of hidden layer and neurons, we tried 21 possible solutions by assuming that we have a single hidden layer, with 2,3,4,5,6,7,8,9,10,12,15,18,20,22,26,28,30,32,36,38, and 40 neurons and ran the program and calculated the ME, MAE, and SDE of the estimated values. Then we tried 50 random combinations of the above number of neurons for two hidden layers and ran the program and calculated ME, MAE, and SDE again. We repeated the same approach for 3 hidden layers. This optimization approach was applied on the entire 220 signal dataset.

Figure 3.8 shows an example of the optimization procedure. Using two separate networks for SBP and DBP, with peak to peak period for systolic and min to min for diastolic as an input. The network for SBP has 3 hidden layers with 1, 3, and 4 neurons, respectively. The network for DBP has 2 hidden layers with 7 and 6 neurons, respectively.

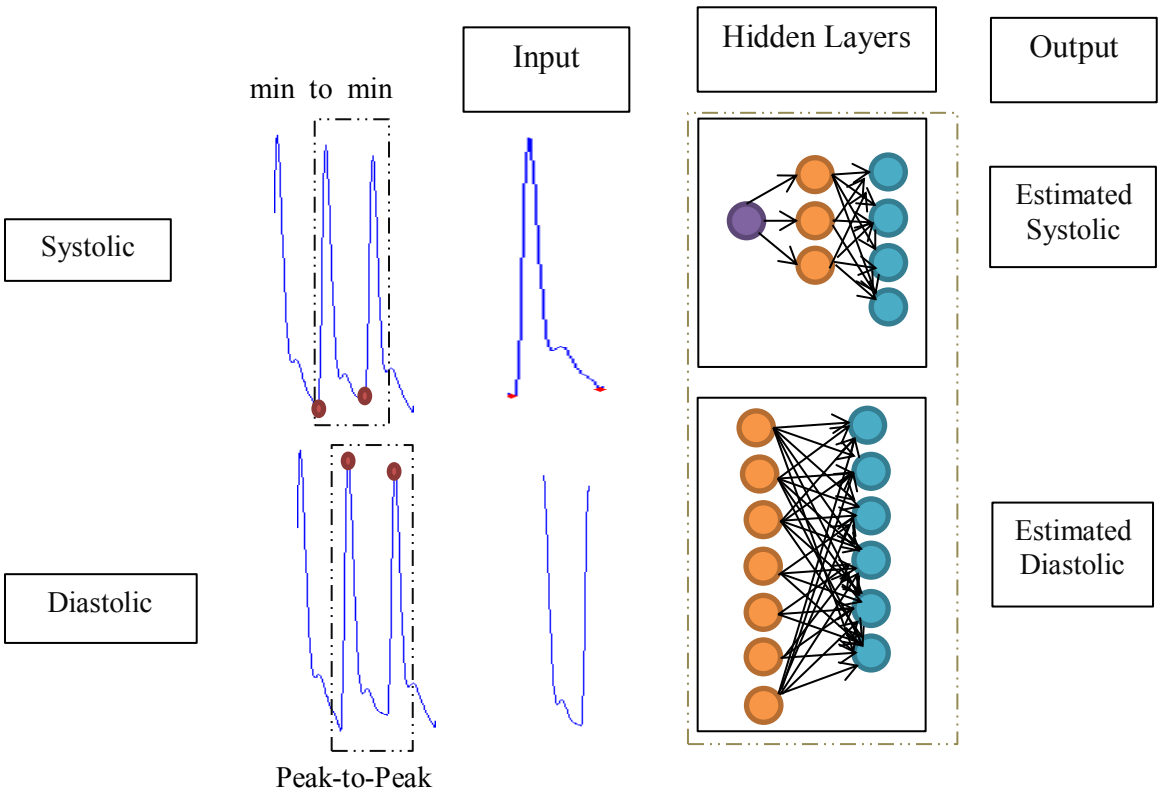

Figure 3.12 From the left to right, top to bottom: (a) An ANN network for systolic BP, one min to min period is selected as input. The training function is L-M backpropagation and the network has 3 hidden layers with 1, 3 and 4 neurons respectively. (b) An ANN network for diastolic BP, one peak to peak period is selected as input. The training function is L-M backpropagation and the network has 2 hidden layers with 7 and 6 neurons respectively.

With the different hidden layers and neurons that were tried, the network that produced the smallest standard deviation of error (SDE) was chosen as the optimized structure for the network in each of the four procedures described in Sections 3.8.1 – 3.8.4 as shown in Table 3.1.

Table 3.1 The optimization of ANN architecture for 4 types of input. SDE is the standard deviation of the error between the estimated value and the reference value obtained from the calibrated ABP waveform (i.e. prior to normalization). The numbers in brackets indicate the number of neurons in each hidden layer.

Input type	Optimized structure		SDE(mmHg)	
	Systolic	Diastolic	Systolic	Diastolic
Raw signal	[8 7 6]	[5 6]	9.64	7.68
Raw Signal + PCA	[2]	[8 7]	5.64	3.21
21 Extracted features	[10 20]	[3 2]	8.58	7.83
21 Extracted Features + PCA	[2 6 9]	[7]	12.73	11.57

4 Results and Discussion

4.1 Results

The performance of our proposed ANN estimation method with different feature sets was evaluated on the dataset of 220 pulses. The feature sets described in Chapter 3 consist of the 1) Raw Signal, 2) PCA of the Raw Signal, 3) 21 Extracted Features and 4) PCA of the 21 Extracted Features. The first feature set of Raw Signal has an input of 100 sample values. The second feature set was obtained by applying principal component analysis (PCA) on the raw signal. For the third features set, we used the 21 features extracted from the raw signal as described in the literature. And for the final feature set, we applied PCA on the 21 Extracted Features. Table 4.1 shows the performance with all four feature sets with the database of 220 pulse periods from 22 patients (11 with normal blood pressure, 11 hypertensive), presented in terms of mean error (ME) and standard deviation of the error (SDE) between estimated SBP and DBP and corresponding reference values. As can be seen, all of the proposed feature sets give estimates that are within the requirements of the ANSI/AAMI standard for non-invasive blood pressure devices, which puts a limit of ±5 mmHg for ME and 8 mmHg for SDE.

Among the four feature sets, applying PCA on the raw signal achieved the best BP estimation results with ME of 0.07 mmHg and SDE of 4.64 mmHg in the estimation of SBP and ME of -0.07 mmHg and SDE of 3.21 mmHg in the estimation of DBP.

As a further test of the performance of the neural network estimation method, and as a check that they have not been over-trained, the networks that were used in the analysis of the 22 patients used for training and testing were fixed (i.e. their architecture and internal weights were fixed). Then 3 new patients with 10 periods each, who are not part of the 22 patient database,

were used as completely "fresh" input data to the network. The result of testing with this fresh data using the four feature sets are also presented in Table 4.1. These results support the finding that the feature set obtained by applying PCA on the raw signal achieves the best BP estimation results with ME of 0.1 mmHg and SDE of 4.84 mmHg in the estimation of SBP, and ME of -0.09 mmHg and SDE of 3.84 mmHg in the estimation of DBP.

Table 4.1 Performance of the ANN with the four tested feature sets. SDE is the Standard Deviation of the Error and ME is the Mean Error.

Signal Type		SDE (mmHg)		ME (mmHg)	
		Systolic	**Diastolic**	**Systolic**	**Diastolic**
Raw Signal	22 Patients	**6.64**	**5.68**	**-0.73**	**-0.45**
	Fresh data (3 patients)	**6.83**	**5.94**	**-0.78**	**-0.56**
Raw Signal + PCA	22 Patients	**4.64**	**3.21**	**0.07**	**-0.07**
	Fresh data (3 patients)	**4.84**	**3.45**	**0.10**	**-0.09**
21Extracted Features	22 Patients	**6.58**	**3.84**	**-1.53**	**0.34**
	Fresh data (3 patients)	**7.03**	**4.10**	**-1.87**	**0.48**
21 Extracted Features + PCA	22 Patients	**7.73**	**4.57**	**0.83**	**0.47**
	Fresh data (3 patients)	**7.88**	**5.01**	**0.85**	**0.57**

4.1.1 Bland-Altman Plots

In order to further analyze the performance of the neural networks with the proposed feature sets, Bland-Altman analysis is performed. Bland and Altman developed a graphical statistical approach to assessing the agreement between a newly developed measurement method and a reference measurement method [80, 81]. Figures 4.1- 4.8 show the Bland–Altman plots that compare the proposed method to the reference measurement with all the feature sets. The reference SBP and DBP (from the invasive ABP signal) are used as targets, and the estimated values of outputs of the neural networks are used as the results of the new measurement method. Each point on the Bland-Altman plot represents the average of the two methods (x-axis) and their difference (y-axis). The horizontal central dashed line shows the bias (ME), while the horizontal dashed lines (above and below the central line) show the limits of agreement (ME±1.96×SDE). Smaller bias and narrower limits of agreements show a better agreement between the two techniques. All plots show two groupings of data, and these relate to the 11 patients with normal blood pressure (on the left), and the 11 patients with hypertension (on the right). Comparing the four plots, it is apparent that the limits of agreement are narrowest in the case of the features obtained by applying PCA on the raw signal for both SBP and DBP estimation.

Compared to the reference values obtained from the invasive method, it is observed that for the features obtained from the raw signal, there is an underestimation of SBP and DBP at pressures in normal blood pressure group, while the results show an overestimation for hypertensive group (Figures 4.1 and 4.2).

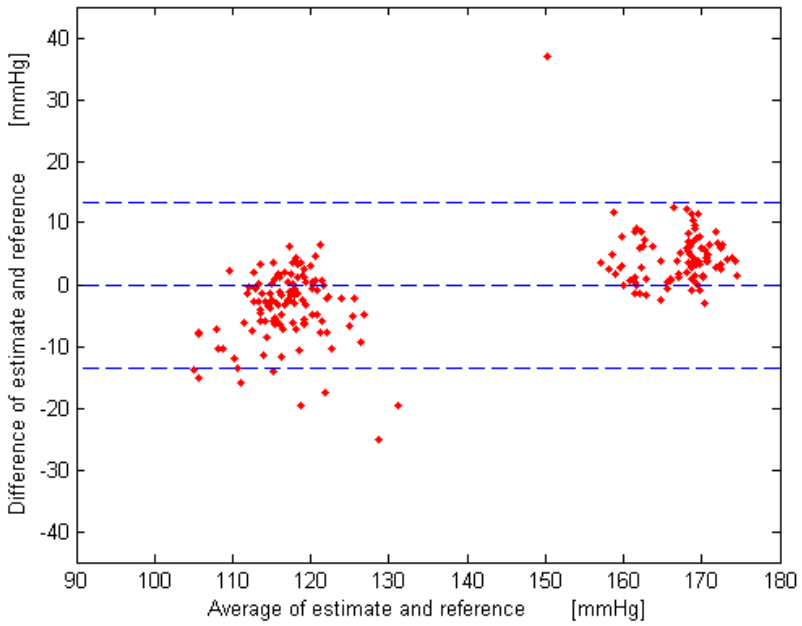

Figure 4.1 The Bland–Altman plot for SBP estimates for the raw signal feature set.

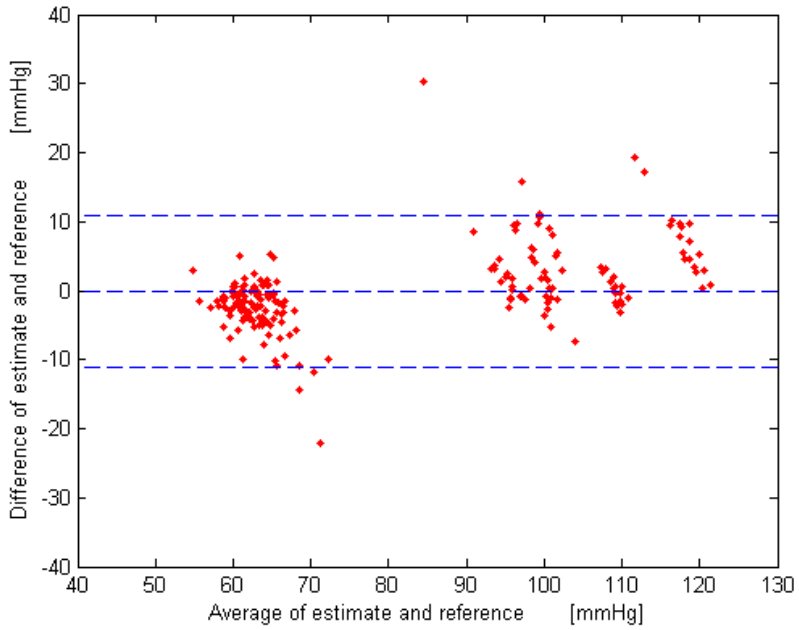

Figure 4.2 The Bland–Altman plot for DBP estimates for the raw signal feature set.

For the test with the feature set obtained by applying PCA on the raw signal, the estimates appear to be better centered around the horizontal zero line compared to the features obtained directly from the raw signal (Figure 4.3 and 4.4 vs. Figure 4.1 and 4.2). However, in each of the normal hypertension and hypertensive groups, there appears to be a slight gradient in the error as the average blood pressure increases.

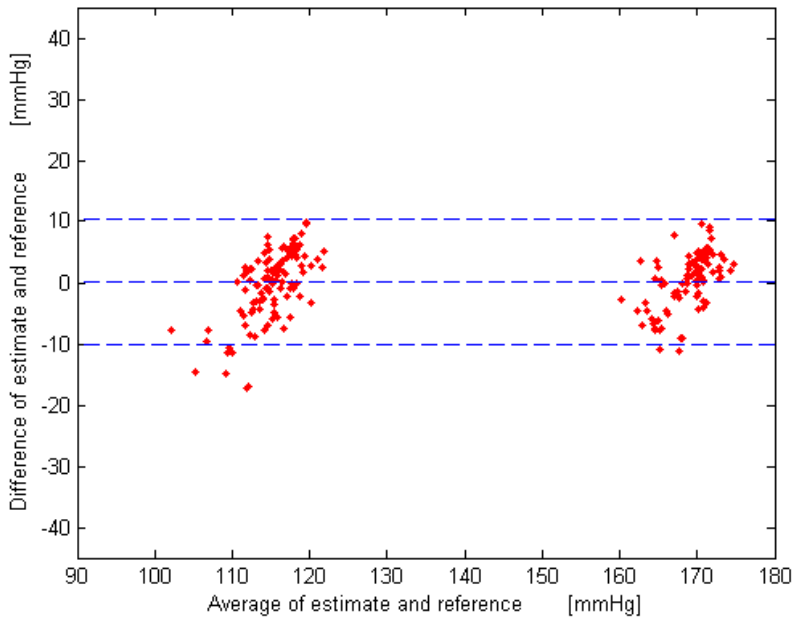

Figure 4.3 The Bland–Altman plot for SBP estimates for feature set obtained by applying the PCA applied on raw signal.

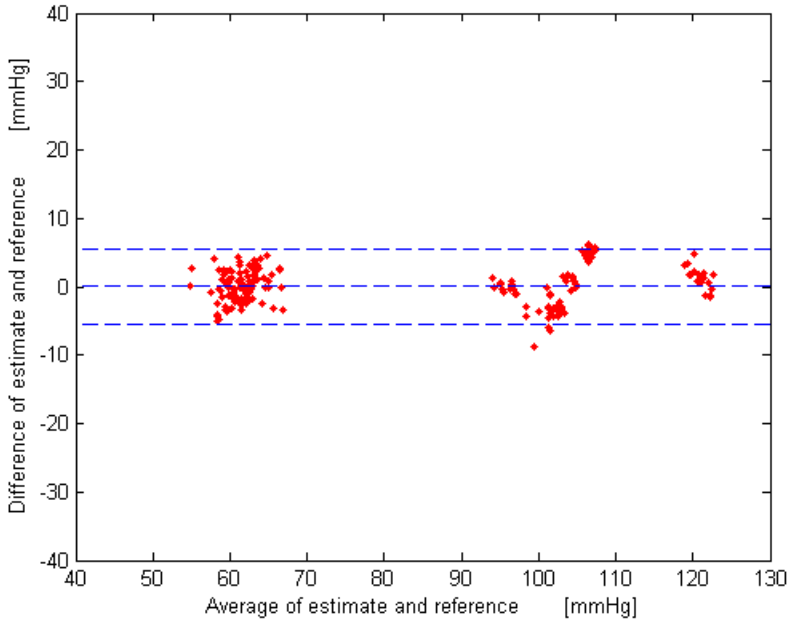

Figure 4.4 The Bland–Altman plot for DBP estimates for feature set obtained by applying the PCA applied on raw signal.

For the 21 extracted features, there is some underestimation of SBP and DBP at pressures for patient in the normal pressure group, and some overestimation of SBP and DBP for the hypertensive patients (Figure 4.5 and 4.6).

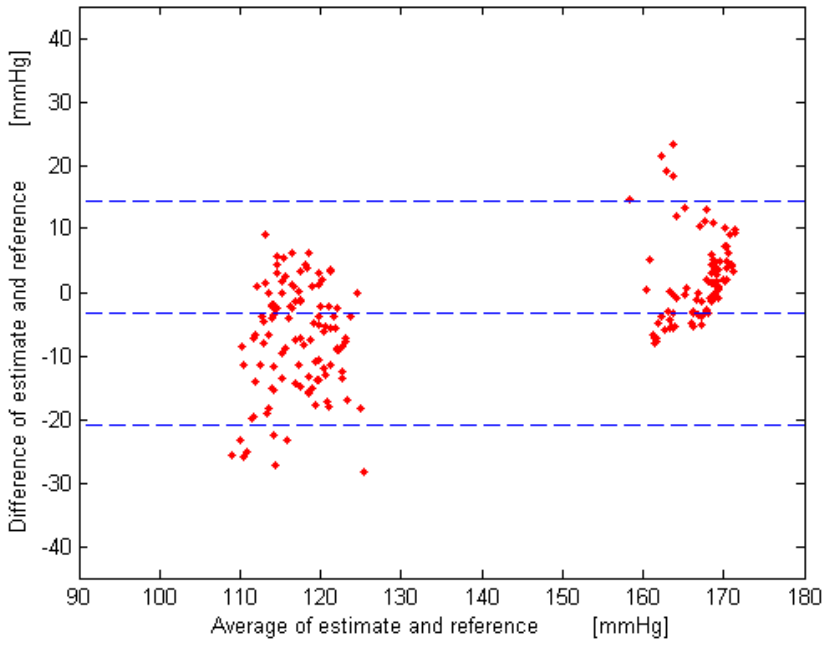

Figure 4.5 The Bland–Altman plot for SBP estimates for the 21 Extracted Features.

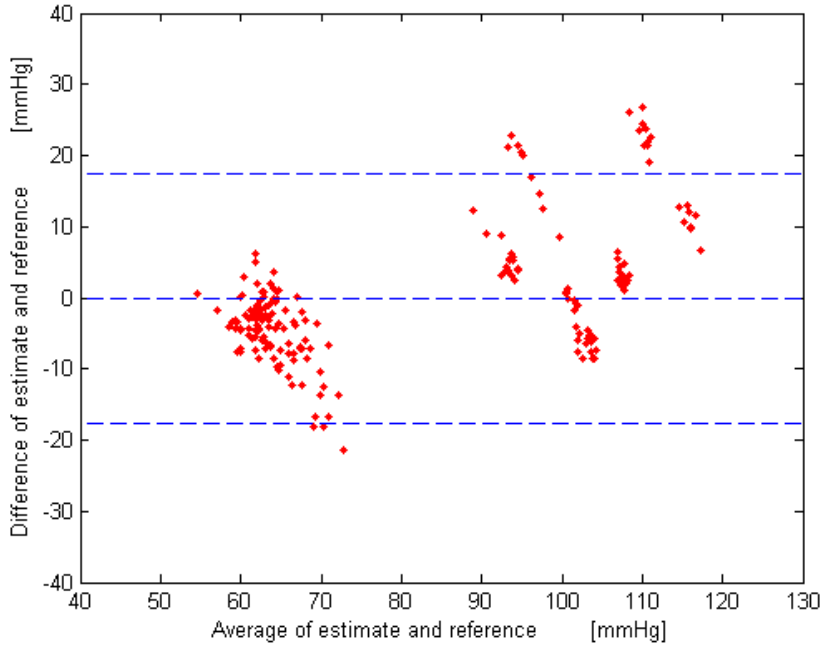

Figure 4.6 The Bland–Altman plot for DBP estimates for the 21 Extracted Features.

For the feature set obtained by applying PCA on the 21 Extracted Features, there is also an underestimation of SBP and DBP in the normal pressure group and an overestimation of SBP and DBP in the hypertensive group (Figure 4.7 and 4.8).

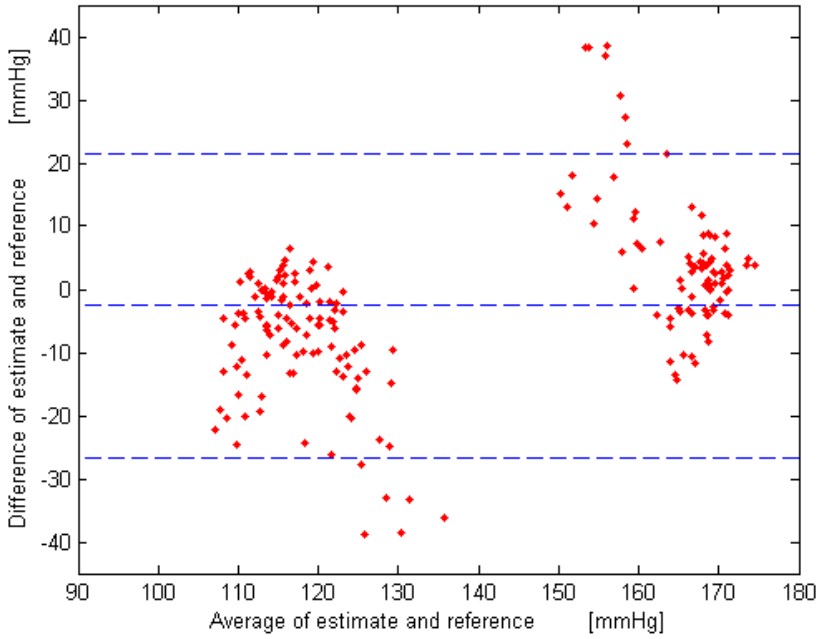

Figure 4.7 The Bland–Altman plot for SBP estimates for features obtained by applying PCA on the 21 Extracted Features.

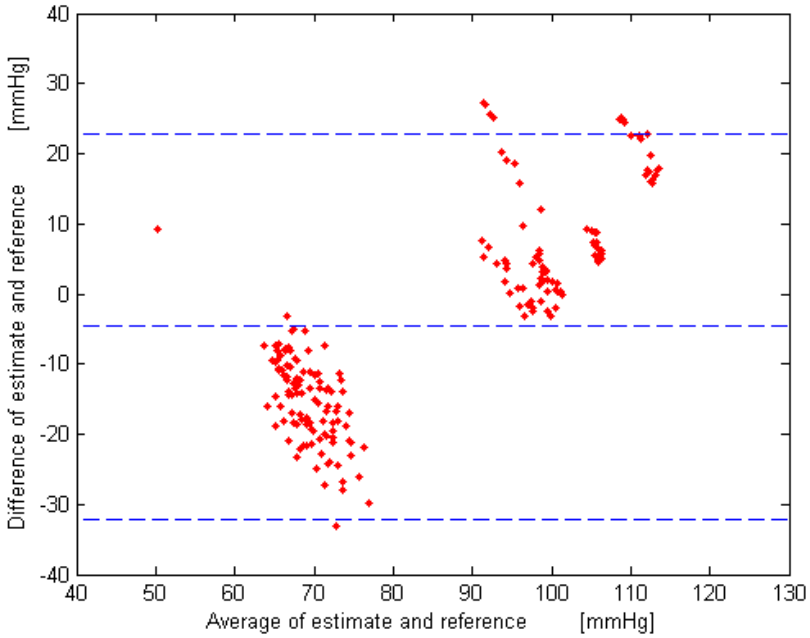

Figure 4.8 The Bland–Altman plot for DBP estimates for features obtained by applying PCA on the 21 Extracted Features.

4.2 Discussion

Table 4.1 summarizes the performance of the neural network approach investigated in this study for the estimation of SBP and DBP from the arterial blood pressure waveform shape. The analysis was done with 4 different feature sets and the results are reported in in terms of ME and SDE. The main observation is that relatively low errors are obtained with this approach, particularly for the case of features obtained by applying PCA on the raw signal. The errors are well within the requirements of the ANSI/AAMI standard for non-invasive measurement of blood pressure.

It can be concluded that in comparison to the raw signal, the dimension reduction method of PCA achieves 0.66 and 0.38 mmHg improvement in terms of ME, and 2.00 and 2.47 mmHg improvement in terms of SDE for SBP and DBP, respectively. The study also found that extracting a set of features suggested in the literature gave poorer results in comparison with using the raw signal, while applying PCA on the extracted features worsens the results further.

As mentioned in Chapter 2, Kurylyak et al. (2013a and 2013b) proposed a method to estimate BP by ANN using the BP waveform, in their case the PPG signal [77, 82]. They used a feedforward ANN with two hidden layers, with 35 and 20 neurons in the first and second hidden layers respectively. More than 5000 pulses from the MIMIC II database were analyzed, and 21 features were extracted from each of them. They obtained a Mean Absolute Error (MAE) of 3.8 mmHg for SBP and 2.21 mmHg for DBP, respectively. The table 4.2 compares the estimation performance for SBP and DBP that we obtained using the same 21 features as used by Kurylyak et al. in terms of MAE. It should be noted that the difference in performance may be due to several reasons. First, the patients and pulses included in the two studies would likely have been different since we chose our patients randomly from a large database. Second, our training set is considerably smaller than in their study, and so their network had a better opportunity to be trained with a large variety of patients with different status (i.e. gender, age, and health status) and pulse shapes. Third, when separating the pulses into the training, validation, and testing sets, it is not clear if Kurylyak et al. separated patients as well, like we did in our study. That is, they may have had pulses from the same patient in each of the three sets, which could augment performance.

Additionally, although they report meeting the requirements of the ANSI/AAMI standard, they evaluate the performance of their method in the form of mean absolute error (MAE) and standard

deviation of absolute error (SDAE) and not mean error (ME) and standard deviation of the error (SDE), as required by the standard.

Never-the-less, even though we obtained larger errors when we used the same 21 features that their study used, it should be noted that the our proposed method which used features obtained by applying PCA on the raw signal resulted in smaller MAE than reported by Kurylyak et al. (4.68 vs. 3.80 mmHg for SBP, and 1.58 vs. 2.21 mmHg for DBP). As a caveat, however, the comparison between the two results might not be completely appropriate, since Kurylyak et al. used pulse waveforms obtained from a PPG sensor to train and test their network, while we used arterial BP waveforms which possibly carry more information related to the blood pressure of the patient.

Table 4.2 Comparison of MAE obtained with by Kurylyak et al. 2013a and our ANN using the same 21 Extracted features.

Signal Type	MAE (mmHg)	
	Systolic	**Diastolic**
21 Extracted Features (our data)	5.20	2.58
21 Extracted Features (Kurylyak et. al, 2013a)	3.80	2.21

The results we have obtained support the potential for developing a cufflesss approach which would be able to measure continuous BP without need of any device calibration, nor need for

recording ECG as is done in the Pulse Arrival Time (PAT) based methods. This approach could potentially be implemented on a smart phone by taking advantage of the light sensor found in it to record the pulse waveform from the finger. Thus there would not be a need to buy separate hardware or/and wearable device. Currently, there is no such application or device available in the market to continuously measure BP without cuff which meets the requirements of any standard such as ANSI/AAMI, European, or British standards.

However an important limitation of the proposed method in terms of developing a cuffless device is that this study relied on invasive waveforms whereas the non-invasive cuffless device would get the waveforms through a surface sensor such as a pulse oximeter which may not contain the same amount of information. On the other hand, using invasive waveforms ensured that the reference values are exact and not obtained through another non-invasive method that has its own errors and noise.

5 Conclusions and Future Work

5.1 Conclusions

The monitoring of vital signs is an important part of monitoring human health status. These days, many major cellphone companies such as Apple, Microsoft, and Samsung are trying to monitor human vital signs via their smartphones [83-85]. However, until now, they have only succeeded in measuring the human pulse and heart rate (HR) through the devices' cameras. Current Apps such as the Samsung HR App or other "Hear Rate" Apps are able to measure the HR with a touch of the index finger using the flash module, or with the camera. Their technology does this by detecting pulsatile changes in finger colour as the result of the blood volume change. It takes approximately 10-20 seconds to measure the HR value and the pulse signal. The principle of the measurement process is the same as the one being used in the pulse oximeter, with the exception that the pulse oximeter has two optical sensors (Red/IR), whereas the camera smartphone has just one sensor, and it uses either yellow or red light [86-88].

The ultimate aim of our project is to develop algorithms to continuously measure BP possibly by using a handheld device such as a smartphone, which could provide the pulse waveform through an optical sensor or through the integrated camera. The algorithms developed and tested in this thesis show that the pulse waveform (at least when measured intra-arterially), contains sufficient information to allow the beat-by-beat estimation of systolic and diastolic pressure.

Unlike most of the cuffless approaches described in the literature, namely those based on measuring PWV, PTT and PAT, the method described in this work uses a computational intelligence approach on only one signal, the arterial pulse waveform, to estimate blood pressure. With the limited set of test data and with the appropriate selection of input features, the Artificial

Neural Network was able to achieve excellent performance, with errors that are considerably smaller than the limits required by the ANSI/AAMI standard for non-invasive measurement of blood pressure. This performance was also consistent for individuals over a wide range of blood pressure values. Another advantage of the method is that it is independent of the person whose vital signs are being measured, and also does not need calibration over time or over subjects since it does not rely on the amplitude of the waveform [72, 89]. If similar results can be achieved with the pulse waveform measured non-invasively, then it can be readily incorporated in smartphone, without the need for an extra device to measure one's vital signs This would be an important contribution to blood pressure monitoring, particularly in the context of home healthcare.

5.2 Contributions

In this thesis, we proposed a novel method based on Artificial Neural Networks to continuously measure cuffless BP without the need of any device calibration, nor the need to record ECG as is done in other published methods based on the PAT. There is no currently available cuffless method or device which meets the requirements of any of the international standards, such as the ANSI/AAMI, European, or British standards. The method was validated with a limited set of patients having a wide range of blood pressures, and achieved very low errors when the input features to the ANN were appropriately selected and processed. The work showed that a good set of such features can be obtained by applying PCA on the samples of the raw signals to reduce the dimensionality of the inputs to the network.

5.3 Limitations

The main limitation of this study is that we used the intra-arterial pulse waveform for training and testing the ANN, and a pulse waveform that is recorded non-invasively may not contain the same information. In particular, the optical PPG sensor of a smartphone will collect the signal from the finger and the finger pulse reflects very peripheral blood vessels far from the heart thereby affecting the shape of the pulse. This effect is illustrated in Figure 5.1, which shows that the shape of the BP signal is different in different peripheral locations. As a result, the current algorithm will likely need to be modified for the PPG signal.

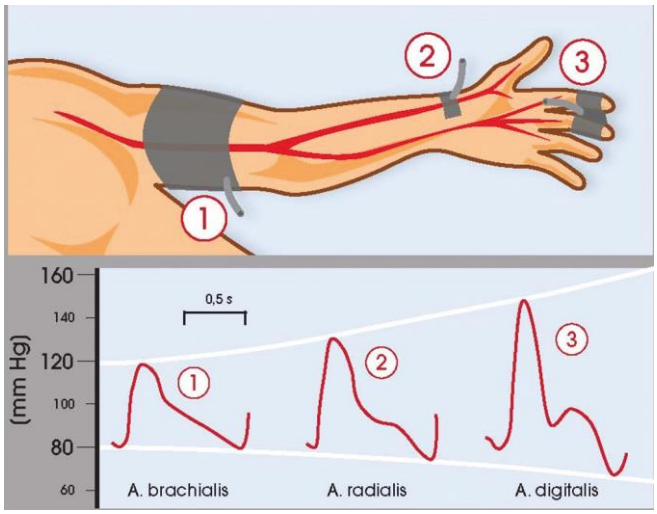

Figure 5.1 Different blood pressure waveforms and amplitudes in the (1) brachialis, (2) radialis and (3) digitalis along the arterial peripheral tree (adapted from [89]).

The second important limitation is that in a real world situation, it is expected there would have several types of noise and artefacts that affect the detected waveform. Therefore, some form of

filtering will likely be required to suppress these artefacts in a preprocessing stage before extracting the signal features. The third limitation of work is that the MIMC database that we used does not have other information about the patients such as gender, age, height, weight, health status and what kind of medications they were using during the measurement. These factors can directly affect the characteristics of the signal and so affect the design and performance of the neural network. A fourth limitation is the concern that the ANN is over-learning because we used all the input signals to optimize the network and ultimately to train the network. However, we mitigated this concern by testing the network with a completely fresh set of data.

Although using the feature set obtained by applying PCA on the raw signal gave very promising results, its usage is limited to particular applications. First, the ANN has a black box structure that implicitly models the relationship between the BP and the pulse signal. For example, it is very difficult to describe the weights at the nodes of the ANN. Therefore, in applications where an explicit relationship between the pulse signal and the BP is required, the use of ANN is limited. Never-the-less, it should be emphasized that in most applications that involve non-invasive blood pressure estimation, characterizing an explicit relationship between the pulse signal and BP is not required. Second, once the ANN has been trained, it is not possible to incorporate additional knowledge such as new data or system settings into the network, without repeating the whole training process. Third, to obtain good results, ANNs require a large training dataset representative of all the target patient population.

5.4 Future work

The next phase of the project will be to use the photoplethysmogram signal (PPG) obtained from the MIMIC II database (Physionet website) as input to the network, and an intra-arterial blood pressure (ABP) signal recorded from the same subject would supply the reference values in the same cardiac cycle. Then, the ANN will be used to train and test the data. However, there are limitations to the MIMIC database such as the aforementioned lack of information regarding the patients. Therefore, we plan to eventually build up our own database which includes the relevant patient information as well as the PPG, ECG, and invasive or non-invasive BP values obtained by trained observers, and covering a variety of patients with a wide range of blood pressures. An ideal database would include 200 healthy subjects, 200 hypertension patients, and 200 patients with other cardiovascular diseases such as peripheral vascular disease (PVD) and premature ventricular contraction [90]. The usage of each individual's information such as health status [70, 72, 75, 90], gender [70], height[70], age [70, 72], weight [70, 72], body mass index [72], heart rate, and oxygen blood concentration [71] could help improve the performance of the algorithm.

The algorithm may encounter difficulties because of differences between the PPG shape and the intra-arterial signal used in this study, and so may require more possessing stages for the input signal before it can be utilized by the neural network. One approach may be to extract appropriate features from PPG signal based on a transfer function between the intra-arterial waveform and the PPG signal. For suppressing noise in the signal, based on the results of the Kurylyak et al. (2013b), using Kalman filtering to remove the low and high-frequency noise may improve the estimation values by up to 20% [82].

For future work, we could also try other machine learning techniques or a combination of them such as ANN and fuzzy systems (or Neuro-Fuzzy systems) [75]. Based on the results shown in [72], other machine learning approaches may be promising.

References

[1] World Health Organization, "A global brief on hypertension: silent killer, global public health crisis: World Health Day 2013," 2013.

[2] World Health Organization, "Causes of death 2008: data sources and methods," 2011.

[3] Hypertension Canada, "Hypertension Canada," 2014.

[4] American standard for electronic and automated sphygmomanometers, ANSI/AAMI SP10 Standard, Arlington, TX, 1993. Bibliography 144.

[5] E. N. Marieb and K. Hoehn, *Human Anatomy & Physiology.* Pearson Education, 2009.

[6] T. G. Pickering, J. E. Hall, L. J. Appel, B. E. Falkner, J. Graves, M. N. Hill, D. W. Jones, T. Kurtz, S. G. Sheps, E. J. Roccella and Subcommittee of Professional and Public Education of the American Heart Association Council on High Blood Pressure Research, "Recommendations for blood pressure measurement in humans and experimental animals: Part 1: blood pressure measurement in humans: a statement for professionals from the Subcommittee of Professional and Public Education of the American Heart Association Council on High Blood Pressure Research," *Hypertension,* vol. 45, pp. 142, 2005.

[7] O. Alexis, "Providing best practice in manual blood pressure measurement," *Br. J. Nurs.,* vol. 18, pp. 410, 2009.

[8] T. Valler-Jones and K. Wedgbury, "Measuring blood pressure using the mercury sphygmomanometer," *Br. J. Nurs.*, vol. 14, pp. 145, 2005.

[9] S. D. Bhatt, A. L. Hinderliter and G. A. Stouffer. Influence of sex on the accuracy of Oscillometric-Derived blood pressures. *The Journal of Clinical Hypertension 13(2),* pp. 112. 2011.

[10] R. A. Peura, "Blood pressure and sound," in *Medical Instrumentation: Application and Design*, 4th ed., J. Webster, Ed. Wiley-India, pp. 297, 2010.

[11] W. Nichols, M. O'Rourke, & C. Vlachopoulos, *McDonald's Blood Flow in Arteries: Theoretical, Experimental and Clinical Principles.* CRC Press, 2011.

[12] J. A. Potkay, "Long term, implantable blood pressure monitoring systems," *Biomed. Microdevices*, vol. 10, pp. 379, 2008.

[13] A. Mosenkis and R. R. Townsend, "Automated Blood Pressure Measurement in Public Places," *The Journal of Clinical Hypertension*, vol. 7, pp. 620, 2005.

[14] S. Buchanan, P. Orris and J. Karliner, "Alternatives to the mercury sphygmomanometer," *J. Public Health Policy*, vol. 32, pp. 107, 2011.

[15] T. G. Papaioannou, A. D. Protogerou, K. S. Stamatelopoulos, M. Vavuranakis and C. Stefanadis, "Non-invasive methods and techniques for central blood pressure estimation: procedures, validation, reproducibility and limitations," *Curr. Pharm. Des.*, vol. 15, pp. 245, 2009.

[16] J. Webster, *Medical Instrumentation: Application and Design.* Wiley-India, 2009.

[17] E. O'Brien, G. Beevers and G. Y. H. Lip, "ABC of hypertension: Blood pressure measurement. Part IV-automated sphygmomanometry: self blood pressure measurement," *BMJ: British Medical Journal*, vol. 322, pp. 1167, 2001.

[18] E. O'Brien, B. Waeber, G. Parati, J. Staessen and M. G. Myers, "Blood pressure measuring devices: recommendations of the European Society of Hypertension," *BMJ*, vol. 322, pp. 531, 2001.

[19] G. C. Carroll, "Blood pressure monitoring," *Crit. Care Clin.*, vol. 4, pp. 411-434, Jul, 1988.

[20] S. Norwood, A. Ruby, J. Civetta and V. Cortes, "Catheter-related infections and associated septicemia." *Chest,* vol. 99, pp. 968, 1991.

[21] E. O'Brien, "Demise of the mercury sphygmomanometer and the dawning of a new era in blood pressure measurement," *Blood Press. Monit.,* vol. 8, pp. 19, 2003.

[22] T. G. Pickering, C. Pieper and C. B. Schechter, *Ambulatory Monitoring and Blood Pressure Variability.* Science Press, 1991.

[23] A. Araghi, J. Bander and J. Guzman, "Arterial blood pressure monitoring in overweight critically ill patients: invasive or noninvasive?" *Critical Care,* vol. 10, pp. R64, 2006.

[24] M. Semret, M. Zidehsarai and R. Agarwal, "Accuracy of oscillometric blood pressure monitoring with concurrent auscultatory blood pressure in hemodialysis patients," *Blood Press. Monit.,* vol. 10, pp. 249, 2005.

[25] D. W. Jones, L. J. Appel, S. G. Sheps, E. J. Roccella and C. Lenfant, "Measuring blood pressure accurately: new and persistent challenges," *JAMA,* vol. 289, pp. 1027, 2003.

[26] A. Bur, H. Herkner, M. Vlcek, C. Woisetschlager, U. Derhaschnig, G. Delle Karth, A. N. Laggner and M. M. Hirschl, "Factors influencing the accuracy of oscillometric blood pressure measurement in critically ill patients," *Crit. Care Med.,* vol. 31, pp. 793, 2003.

[27] U. Tholl, K. Forstner and M. Anlauf, "Measuring blood pressure: pitfalls and recommendations," *Nephrology Dialysis Transplantation,* vol. 19, pp. 766, 2004.

[28] D. W. McKay, N. R. Campbell, L. S. Parab, A. Chockalingam and J. G. Fodor, "Clinical assessment of blood pressure." *J. Hum. Hypertens.,* vol. 4, pp. 639, 1990.

[29] G. Van Montfrans, G. Van Der Hoeven, J. Karemaker, W. Wieling and A. Dunning, "Accuracy of auscultatory blood pressure measurement with a long cuff." *Br. Med. J. (Clin. Res. Ed),* vol. 295, pp. 354, 1987.

[30] T. G. Pickering, "Blood pressure measurement and detection of hypertension," *The Lancet*, vol. 344, pp. 31, 1994.

[31] F. S. Cattivelli and H. Garudadri, "Noninvasive cuffless estimation of blood pressure from pulse arrival time and heart rate with adaptive calibration," in *Wearable and Implantable Body Sensor Networks, 2009. BSN 2009. Sixth International Workshop On*, pp. 114, 2009.

[32] G. Mancia, M. Bombelli, R. Facchetti, F. Madotto, G. Corrao, F. Q. Trevano, G. Grassi and R. Sega, "Long-term prognostic value of blood pressure variability in the general population: results of the Pressioni Arteriose Monitorate e Loro Associazioni Study," *Hypertension*, vol. 49, pp. 1265, 2007.

[33] M. P. Devbhandari, Z. Shariff and A. J. Duncan, "Skin necrosis in a critically ill patient due to a blood pressure cuff," *J. Postgrad. Med.*, vol. 52, pp. 136, 2006.

[34] R. A. Reeves, "Does This Patient Have Hypertension?" *JAMA: The Journal of the American Medical Association*, vol. 273, pp. 1211, 1995.

[35] T. G. Pickering, W. Gerin, J. E. Schwartz, T. M. Spruill and K. W. Davidson, "Franz Volhard lecture: should doctors still measure blood pressure? The missing patients with masked hypertension," *J. Hypertens.*, vol. 26, pp. 2259, 2008.

[36] G. Parati, L. R. Krakoff and P. Verdecchia, "Methods of measurements: home and ambulatory blood pressure monitoring," *Blood Press. Monit.*, vol. 15, pp. 100, 2010.

[37] T. Akpolat, M. Dilek, T. Aydogdu, Z. Adibelli, D. G. Erdem and E. Erdem, "Home sphygmomanometers: validation versus accuracy," *Blood Press. Monit.*, vol. 14, pp. 26, 2009.

[38] M. G. Myers, M. Valdivieso, A. Kiss and S. W. Tobe, "Comparison of two automated sphygmomanometers for use in the office setting," *Blood Press. Monit.*, vol. 14, pp. 45, 2009.

[39] M. Stolt, G. Sjonell, H. Astrom, S. Rossner and L. Hansson, "Improved accuracy of indirect blood pressure measurement in patients with obese arms," *Am. J. Hypertens.*, vol. 6, pp. 66, 1993.

[40] P. E. Nielsen, B. Larsen, P. Holstein and H. L. Poulsen, "Accuracy of auscultatory blood pressure measurements in hypertensive and obese subjects," *Hypertension*, vol. 5, pp. 122, 1983.

[41] G. Smith, "Device Bullentin- Blood Pressure Monitoring Devices," 2006.

[42] T. G. Pickering, "The case for a hybrid sphygmomanometer," *Blood Press. Monit.*, vol. 6, pp. 177, 2001.

[43] M. J. Burke, H. M. Towers, K. O'Malley, D. J. Fitzgerald and E. T. O'Brien, "Sphygmomanometers in hospital and family practice: problems and recommendations." *Br. Med. J. (Clin. Res. Ed)*, vol. 285, pp. 469, 1982.

[44] R. H. Bailey, V. L. Knaus and J. H. Bauer, "Aneroid sphygmomanometers: an assessment of accuracy at a university hospital and clinics," *Arch. Intern. Med.*, vol. 151, pp. 1409, 1991.

[45] V. J. Canzanello, P. L. Jensen and G. L. Schwartz, "Are aneroid sphygmomanometers accurate in hospital and clinic settings?" *Arch. Intern. Med.*, vol. 161, pp. 729, 2001.

[46] D. Mion and A. M. Pierin, "How accurate are sphygmomanometers?" *J. Hum. Hypertens.*, vol. 12, pp. 245, 1998.

[47] S. A. Yarows and K. Qian, "Accuracy of aneroid sphygmomanometers in clinical usage: University of Michigan experience," *Blood Press. Monit.*, vol. 6, pp. 101, 2001.

[48] F. Tasker, A. De Greeff and A. Shennan, "Development and validation of a blinded hybrid device according to the European Hypertension Society protocol: Nissei DM-3000," *J. Hum. Hypertens.*, vol. 24, pp. 609, 2010.

[49] G. S. Stergiou, P. P. Giovas, C. P. Gkinos and D. G. Tzamouranis, "Validation of the A&D UM-101 professional hybrid device for office blood pressure measurement according to the International Protocol," *Blood Press. Monit.,* vol. 13, pp. 37, 2008.

[50] T. G. Pickering, "What will replace the mercury sphygmomanometer?" *Blood Press. Monit.,* vol. 8, pp. 23, 2003.

[51] G. W. Mauck, C. R. Smith, L. A. Geddes and J. D. Bourland, "The meaning of the point of maximum oscillations in cuff pressure in the indirect measurement of blood pressure—part ii," *J. Biomech. Eng.,* vol. 102, pp. 28, 1980.

[52] G. A. Van Montfrans, "Oscillometric blood pressure measurement: progress and problems," *Blood Press. Monit.,* vol. 6, pp. 287, 2001.

[53] J. M. Mallion, J. P. Baguet and G. Mancia, "European Society of Hypertension Scientific Newsletter: Clinical value of ambulatory blood pressure monitoring," *J. Hypertens.,* vol. 24, pp. 2327, 2006.

[54] A. Charmoy, G. Wurzner, C. Ruffieux, C. Hasler, F. Cachat, B. Waeber and M. Burnier, "Reactive rise in blood pressure upon cuff inflation: cuff inflation at the arm causes a greater rise in pressure than at the wrist in hypertensive patients," *Blood Press. Monit.,* vol. 12, pp. 275, 2007.

[55] N. McGowan and P. L. Padfield, "Self blood pressure monitoring: a worthy substitute for ambulatory blood pressure&quest," *J. Hum. Hypertens.,* vol. 24, pp. 801, 2010.

[56] T. H. Westhoff, H. Straub-Hohenbleicher, S. Schmidt, M. Tölle, W. Zidek and M. Giet, "Convenience of ambulatory blood pressure monitoring: comparison of different devices," *Blood Press. Monit,* vol. 10, pp. 239, 2005.

[57] L. R. Krakoff, "Cost-Effectiveness of Ambulatory Blood Pressure," *Hypertension,* vol. 47, pp. 29, 2006.

[58] World Health Organization, and International Society of Hypertension Writing Group, "2003 World Health Organization (WHO)/International Society of Hypertension (ISH) statement on management of hypertension," vol. 21, pp. 1983, 2003.

[59] C. C. Y. Poon, Y. M. Wong and Y. T. Zhang, "M-health: The development of cuff-less and wearable blood pressure meters for use in body sensor networks," *Life Science Systems and Applications Workshop, 2006. IEEE/NLM,* pp. 1, 2006.

[60] C. C. Y. Poon and Y. T. Zhang, "Cuff-less and noninvasive measurements of arterial blood pressure by pulse transit time," *Engineering in Medicine and Biology Society, 2005. IEEE-EMBS 2005. 27th Annual International Conference of The IEEE,* pp. 5877, 2005

[61] J. Espina, T. Falck, J. Muehlsteff and X. Aubert, "Wireless body sensor network for continuous cuff-less blood pressure monitoring," *Medical Devices and Biosensors, 2006. 3rd IEEE/EMBS International Summer School On,* pp. 11, 2006.

[62] J. Muehlsteff, X. L. Aubert and M. Schuett, "Cuffless estimation of systolic blood pressure for short effort bicycle tests: The prominent role of the pre-ejection period," *Engineering in Medicine and Biology Society, 2006. EMBS'06. 28th Annual International Conference of the IEEE,* pp. 5088, 2006.

[63] J. Muehlsteff, X. A. Aubert and G. Morren, "Continuous cuff-less blood pressure monitoring based on the pulse arrival time approach: The impact of posture," *Engineering in Medicine and Biology Society, 2008. EMBS 2008. 30th Annual International Conference of the IEEE,* pp. 1691, 2008.

[64] J. C. Bramwell and A. V. Hill, "The Velocity of the Pulse Wave in Man," *Proceedings of the Royal Society of London. Series B, Containing Papers of a Biological Character*, pp. 298, 1922.

[65] D. J. Hughes, C.F. Babbs, L. A. Geddes and J. D. Bourland, "Measurement of Young's modulus of elasticity of the canine aorta with ultrasound," *Ultrasonic Imaging*, vol. 1, pp. 356, 1979.

[66] W. Chen, T. Kobayashi, S. Ichikawa, Y. Takeuchi and T. Togawa, "Continuous estimation of systolic blood pressure using the pulse transit time and intermittent calibration," *Medical and Biological Engineering and Computing*, vol. 38, pp. 567, 2000.

[67] Y. T. Zhang , C. C.Y Poon, C. H. Chan, M. W. W. Tsang, and K. F. Wu, "A health-shirt using e-textile materials for the continuous and cuffless monitoring of arterial blood pressure," *Medical Devices and Biosensors, 2006. 3rd IEEE/EMBS International Summer School on*, pp. 86, 2006.

[68] W. B. Gu, C. C. Y. Poon, M. Y. Sy, H. K. Leung, Y. P. Liang and Y. T. Zhang, "A h-Shirt-Based Body Sensor Network for Cuffless Calibration and Estimation of Arterial Blood Pressure," *2009 Body Sensor Networks*, pp. 151, 2009.

[69] J. Espina, T. Falck, J. Muehlsteff, Y. Jin, M. A. Adan and X. Aubert, "Wearable body sensor network towards continuous cuff-less blood pressure monitoring," *Medical Devices and Biosensors, 2008. ISSS-MDBS 2008. 5th International Summer School and Symposium On*, pp. 28, 2008.

[70] S. Suzuki and K. Oguri, "Cuffless blood pressure estimation by error-correcting output coding method based on an aggregation of AdaBoost with a photoplethysmograph sensor,"

Engineering in Medicine and Biology Society, 2009. EMBC 2009. Annual International Conference of the IEEE, pp. 6765, 2009.

[71] V. Abouei, H. Sharifian, F. Towhidkhah, V. R. Nafisi, and H. Abouie, "Using neural network in order to predict hypotension of hemodialysis patients," *Electrical Engineering (ICEE), 2011 19th Iranian Conference on*, vol. 19, pp. 1, 2011.

[72] E. Monte-Moreno, "Non-invasive estimate of blood glucose and blood pressure from a photoplethysmograph by means of machine learning techniques," *Artif. Intell. Med.*, vol. 53, pp. 127, Oct, 2011.

[73] K. L. Priddy and P. E. Keller, *Artificial Neural Networks: An Introduction*. SPIE Press, 2005.

[74] J. A. Reggia, "Neural computation in medicine," *Artif. Intell. Med.*, vol. 5, pp. 143, 1993.

[75] M. Soltane, M. Ismail, and Z. A. Abdul Rashid., "Artificial Neural Networks (ANN) Approach to PPG Signal Classification," *International Journal of Computing & Information Sciences 2*, vol. 2, pp. 58, 2004.

[76] Association for the Advancement of Medical Instrumentation. American National Standard. Manual, electronic or automated sphygmomanometers ANSI/AAMI SP10-2002/A1. 3330 Washington Boulevard, Suite 400, Arlington, VA 22201-4598, USA: AAMI; 2006.

[77] Y. Kurylyak, F. Lamonaca, and D. Grimaldi, "A neural network-based method for continuous blood pressure estimation from a PPG signal," *Instrumentation and Measurement Technology Conference (I2MTC), 2013 IEEE International*, vol. 12, pp. 280, 2013.

[78] X. F. Teng and Y. T. Zhang., "Continuous and noninvasive estimation of arterial blood pressure using a photoplethysmographic approach," *Engineering in* M*edicine and Biology*

Society, 2003. Proceedings of the 25th Annual International Conference of the IEEE, vol. 4, pp. 3153, 2003.

[79] S. P. Linder, S. M. Wendelken, E. Wei, and S. P. McGrath., "Using the morphology of photoplethysmogram peaks to detect changes in posture," *posture.Journal of clinical monitoring and computing,* vol. 20, pp. 151, 2006.

[80] D. G. Altman and J. M. Bland., "Measurement in medicine: the analysis of method comparison studies," *The statistician,* pp. 307, 1983.

[81] J. M. Bland and D. G. Altman., "Statistical methods for assessing agreement between two methods of clinical measurement," *The lancet,* vol. 327, pp. 307, 1986.

[82] Y. Kurylyak, K. Barbe, F. Lamonaca, D. Grimaldi, and W. V. Moer, "Photoplethysmogram-based Blood pressure evaluation using Kalman filtering and Neural Networks," *Medical Measurements and Applications Proceedings (MeMeA), 2013 IEEE International Symposium on,* pp. 170, 2013.

[83] M. Gurman, *This is Healthbook, Apple's major first step into health & fitness tracking*. Available: http://9to5mac.com/2014/03/17/this-is-healthbook-apples-first-major-step-into-health-fitness-tracking/.

[84] P. Pachal, *How the Samsung Galaxy S5 Measures Your Heart Rate.* Available: http://mashable.com/2014/02/25/samsung-gs5-heart-rate/.

[85] N. Tue. *Manage your personal health records with lumia.* Available: http://conversations.nokia.com/2014/09/02/manage-personal-health-records-lumia/.

[86] K. Matsumura, P. Rolfe, J. Lee and T. Yamakoshi, "iPhone 4s Photoplethysmography: Which Light Color Yields the Most Accurate Heart Rate and Normalized Pulse Volume Using

the iPhysioMeter Application in the Presence of Motion Artifact?" *PloS One,* vol. 9, pp. 91205, 2014.

[87] M. J. Gregoski, M. Mueller, A. Vertegel, A. Shaporev, B. B. Jackson, R. M. Frenzel, S. M. Sprehn and F. A. Treiber, "Development and validation of a smartphone heart rate acquisition application for health promotion and wellness telehealth applications," *International Journal of Telemedicine and Applications,* vol. 2012, pp. 1, 2012.

[88] E. Jonathan and M. Leahy, "Investigating a smartphone imaging unit for photoplethysmography," *Physiol. Meas.,* vol. 31, pp. N79, 2010.

[89] E. Sackl-Pietsch, "Continuous non-invasive arterial pressure shows high accuracy in comparison to invasive intra-arterial blood pressure measurement," *Unpublished manuscript,* 2010.

[90] M. A. Allen, "Development of a neural network screening aid for diagnosing lower limb peripheral vascular disease from photoelectric plethysmography pulse waveforms," *Physiol. Meas.* , vol. 14, pp. 13, 1993.

Appendix

Table A-1 – Blood Pressure Estimation Results in Individual Pulse Waveforms. Reference values of SBP and DBP and estimates obtained using Artificial Neural Networks based on 4 feature sets for each individual pulse from 22 patients. See text for details on the feature sets.

Abbreviations: Est.: Estimated, PCA: Principal Component Analysis, EF: Extracted Features.

	SBP					DBP				
	Ref.	Est. Raw	Est. Raw + PCA	Est. 21EF	Est. 21EF+ PCA	Ref.	Est. Raw	Est. Raw + PCA	Est. 21EF	Est. 21EF + PCA
1	121.72	131.10	115.57	121.73	131.90	60.86	59.76	59.61	77.61	85.21
2	121.72	121.01	114.61	125.65	136.66	61.45	63.92	60.70	73.74	81.64
3	119.57	119.30	113.52	113.25	113.24	61.45	66.07	59.19	65.55	71.62
4	122.90	125.03	120.47	117.19	122.85	62.23	67.21	60.17	70.90	82.60
5	122.90	118.38	114.96	119.67	123.26	60.27	64.08	61.92	71.50	77.99
6	122.90	127.94	119.12	121.14	123.87	61.25	75.57	58.83	79.28	81.31
7	124.46	126.59	114.67	119.42	119.46	63.99	67.05	60.82	76.61	77.47
8	124.46	129.33	114.81	124.56	134.01	60.27	70.49	60.55	72.61	81.04
9	121.33	140.89	114.26	126.95	121.10	60.08	82.19	55.91	78.21	79.32
10	124.46	117.97	119.22	118.38	124.82	63.21	63.21	59.47	67.50	80.02

11	114.68	120.84	120.41	124.03	122.96	58.12	61.07	59.71	65.49	76.53
12	116.44	119.36	116.39	131.73	147.87	59.69	63.55	59.82	69.84	87.64
13	116.44	122.00	115.18	128.91	141.36	59.69	62.12	59.62	69.41	83.98
14	115.85	118.30	115.53	129.43	128.79	60.27	59.61	60.62	69.64	78.59
15	113.89	118.77	114.75	124.78	134.36	59.88	62.36	61.27	68.47	83.87
16	118.40	124.37	121.81	125.22	145.02	60.27	62.03	59.53	67.13	86.95
17	119.77	118.24	115.55	124.11	128.66	59.69	63.59	57.32	64.30	78.31
18	119.77	118.68	114.14	123.55	129.35	60.08	60.55	58.25	64.00	77.89
19	117.81	117.60	114.69	123.32	122.49	58.51	59.63	59.01	64.22	77.05
20	115.46	116.54	115.06	122.40	122.04	59.69	59.91	59.04	65.55	76.84
21	111.55	115.68	114.62	122.97	139.21	57.93	59.14	60.78	61.34	79.52
22	110.18	118.61	114.99	124.97	123.38	55.77	58.24	60.88	63.40	74.60
23	108.02	122.19	116.62	121.47	130.48	56.16	62.99	60.51	63.83	79.55
24	111.15	115.73	118.10	115.15	111.95	57.73	61.41	61.14	60.81	73.74
25	111.15	112.50	114.45	139.56	149.61	57.93	59.52	60.79	66.39	82.89
26	110.57	116.61	114.82	115.23	114.24	57.73	60.28	61.34	62.33	72.46
27	108.61	116.23	114.12	115.19	113.18	56.16	61.53	61.06	57.92	72.23

28	108.41	114.63	117.21	121.82	145.24	57.73	63.43	61.36	62.09	84.91
29	112.13	118.55	118.15	121.89	134.70	59.49	63.34	61.00	64.03	82.30
30	112.13	118.09	115.06	129.26	122.49	59.49	60.40	61.77	66.70	73.91
31	115.07	114.84	114.13	115.28	125.01	60.08	60.69	60.84	62.80	79.69
32	117.03	113.44	114.53	116.17	126.22	59.49	61.18	58.51	61.83	77.35
33	117.03	118.73	117.92	121.05	134.03	58.32	59.12	58.71	63.53	79.93
34	114.09	117.40	115.00	118.05	120.38	57.14	58.64	58.05	60.65	79.34
35	114.09	115.55	116.73	111.62	110.15	57.14	59.26	59.68	61.45	75.26
36	116.05	141.21	112.65	117.48	129.98	54.99	56.43	54.78	54.29	45.65
37	116.05	118.59	114.12	134.17	139.60	56.36	53.32	53.61	60.56	89.38
38	115.85	115.02	116.67	115.12	123.04	56.36	66.23	60.34	63.56	77.30
39	115.85	122.34	118.16	115.99	120.31	59.10	63.52	60.38	64.48	80.46
40	113.11	114.44	113.53	117.43	117.64	58.71	61.17	61.79	63.10	75.63
41	119.37	115.79	113.60	126.74	124.42	64.19	63.36	61.56	64.19	75.81
42	117.61	118.29	114.63	126.37	153.75	63.99	64.99	62.27	64.69	84.87
43	116.63	118.32	114.28	121.62	121.12	61.84	65.67	61.48	58.87	82.95
44	117.61	122.55	117.70	125.03	124.52	65.17	63.71	62.47	64.14	79.15

45	120.94	123.12	115.16	126.60	129.92	64.97	65.42	61.09	64.13	78.44
46	120.94	120.40	115.49	123.34	129.66	64.77	66.22	62.22	62.74	78.43
47	118.98	117.72	114.96	124.73	125.25	64.38	62.86	61.64	64.45	76.91
48	117.22	116.95	114.89	122.31	122.96	64.38	63.47	62.27	59.25	81.03
49	119.96	120.56	118.12	123.51	128.21	65.95	67.47	61.83	62.24	82.97
50	119.96	116.73	114.71	122.12	119.42	64.97	64.20	61.91	58.89	78.50
51	118.40	123.20	110.94	127.07	115.83	61.84	65.97	62.56	64.38	73.83
52	114.48	121.76	113.87	126.48	116.15	60.08	62.75	62.83	65.51	74.53
53	111.35	114.12	115.64	126.57	114.91	60.67	61.03	62.31	62.52	74.79
54	112.92	116.14	113.39	126.39	112.66	61.45	61.24	62.59	63.28	73.85
55	114.09	117.21	115.50	126.75	111.97	61.45	64.18	62.91	62.61	75.49
56	117.61	120.07	119.83	127.07	114.39	62.82	64.05	62.67	65.06	76.30
57	117.61	115.69	111.44	126.74	113.76	62.23	62.43	62.67	64.93	74.40
58	115.46	117.16	113.59	126.95	114.11	61.06	61.89	62.78	64.26	73.89
59	112.72	118.19	115.21	126.55	114.19	59.69	62.57	63.16	62.51	73.70
60	112.92	119.26	117.71	126.34	116.54	60.86	66.00	63.30	63.14	74.39
61	117.61	118.95	116.26	113.00	113.97	62.43	64.69	62.83	63.61	70.17

62	117.61	120.91	115.82	108.57	116.50	60.27	64.68	62.83	62.14	69.96
63	116.05	122.27	114.36	115.12	116.96	60.27	61.10	59.30	66.95	71.96
64	116.63	117.72	112.84	114.28	115.22	63.01	62.86	62.84	64.12	70.71
65	116.63	115.42	111.74	112.39	113.59	61.45	65.24	63.42	63.22	70.26
66	118.20	126.04	118.45	113.63	114.64	61.84	60.93	61.37	64.99	72.20
67	118.20	116.61	114.74	112.77	113.63	63.01	62.35	62.13	62.12	71.18
68	116.83	114.99	114.89	114.24	114.62	62.23	60.58	62.23	62.56	70.39
69	117.42	125.16	118.32	112.37	119.33	61.45	60.90	61.59	62.95	68.81
70	117.42	127.83	111.94	111.79	119.52	60.08	64.13	61.82	64.54	67.42
71	121.14	123.17	114.60	119.15	123.34	60.67	62.20	58.49	63.60	72.52
72	120.35	121.24	116.29	115.90	119.18	63.21	67.37	58.90	62.45	74.31
73	120.35	114.16	114.74	115.95	117.43	60.08	61.63	59.42	59.93	71.00
74	120.35	120.03	117.59	118.28	132.67	64.77	63.93	61.56	63.44	76.16
75	120.35	115.96	115.27	119.17	123.62	60.47	61.96	60.77	62.45	71.30
76	120.35	117.89	115.72	115.89	118.21	60.47	59.82	58.08	62.85	72.71
77	120.35	116.92	115.37	116.46	122.39	61.45	63.10	62.12	62.81	74.50
78	121.53	121.73	118.74	117.92	132.45	62.82	63.11	59.57	66.47	78.37

79	121.53	118.55	114.20	115.39	117.29	63.01	63.66	61.42	62.80	72.17
80	121.53	128.36	117.21	118.50	132.41	67.12	77.17	62.51	67.01	79.50
81	103.13	118.93	120.47	121.83	118.30	60.08	65.37	61.75	64.47	70.85
82	98.04	113.08	112.59	121.59	117.25	60.27	71.14	62.81	60.00	70.83
83	98.24	111.99	106.05	122.58	117.75	65.17	70.95	68.62	72.24	73.29
84	104.31	116.24	114.96	121.31	118.40	60.08	67.81	62.17	66.24	69.55
85	104.31	111.55	115.68	121.41	114.68	63.01	73.92	65.39	60.92	72.57
86	101.76	109.65	116.72	123.29	118.71	63.99	70.40	67.13	70.97	75.02
87	101.76	109.75	111.49	125.45	122.31	61.25	66.17	61.32	63.87	69.40
88	102.94	113.26	110.67	122.85	116.02	61.25	67.77	62.92	68.52	73.90
89	103.72	113.99	120.56	123.47	122.08	62.04	64.16	63.77	66.38	69.24
90	103.72	117.35	115.17	127.92	120.89	60.47	63.54	62.29	63.32	70.04
91	110.76	108.63	110.69	114.68	109.64	63.80	61.44	62.75	70.89	79.75
92	112.92	115.56	114.68	116.84	116.71	64.97	66.62	63.79	68.74	68.17
93	112.92	116.35	110.33	115.75	110.07	64.97	65.55	65.11	71.00	81.05
94	112.92	120.07	120.34	116.06	113.54	64.97	68.04	65.11	68.32	69.92
95	112.92	116.77	110.84	114.84	112.97	64.58	76.37	64.58	66.33	69.78

96	108.81	128.51	113.43	118.17	112.42	64.58	67.89	64.69	75.07	83.45
97	112.52	118.49	115.37	116.92	112.62	66.34	65.02	64.54	69.54	71.56
98	112.52	113.18	112.08	115.97	110.46	66.54	69.38	66.75	68.59	80.56
99	113.11	123.80	118.66	114.52	110.49	67.71	62.80	65.13	71.26	75.09
100	113.11	130.55	111.06	120.54	113.79	67.51	62.24	65.17	74.20	78.91
101	113.11	130.55	111.06	120.54	113.79	67.51	62.24	65.17	74.20	78.91
102	113.31	113.18	111.17	115.86	113.20	63.21	58.29	61.09	64.01	81.51
103	111.15	117.03	112.24	128.23	116.33	65.36	67.47	64.54	79.06	87.29
104	115.07	118.26	115.25	119.90	120.09	63.99	64.61	62.89	71.13	82.16
105	115.07	111.85	111.39	117.63	116.24	62.04	66.67	62.87	69.90	80.13
106	108.22	119.62	115.10	127.52	121.37	62.04	71.40	61.05	83.39	91.95
107	113.70	116.09	117.24	119.92	118.66	62.62	65.57	62.75	70.48	82.22
108	113.70	111.67	111.45	121.97	118.37	63.01	67.20	62.43	76.75	86.12
109	110.37	121.97	118.09	118.87	115.97	63.99	68.64	62.63	72.44	85.15
110	111.94	114.61	114.99	119.87	117.73	62.62	63.50	62.91	69.12	77.71
111	111.94	112.23	110.88	130.07	118.06	62.62	69.43	62.41	79.39	88.79
112	175.34	169.51	171.57	161.80	163.74	120.35	115.73	117.25	101.33	103.46

113	175.34	168.50	168.11	165.16	166.46	120.94	118.20	117.50	108.18	103.39
114	171.23	167.41	168.10	166.56	171.27	120.55	120.19	118.88	109.94	104.58
115	175.34	173.87	173.26	166.43	171.11	120.55	115.05	118.71	113.92	104.83
116	176.13	171.67	166.98	166.36	171.46	122.50	117.29	117.60	110.82	104.61
117	176.13	167.48	167.05	166.70	171.24	122.11	119.13	120.78	109.13	104.56
118	171.04	165.62	167.92	166.11	171.29	120.94	117.52	117.50	110.96	104.61
119	176.32	172.39	173.23	165.39	166.66	120.94	116.35	122.18	111.24	103.53
120	175.93	169.53	167.40	166.49	172.49	121.72	120.91	120.00	109.78	104.72
121	162.04	163.65	173.21	165.54	144.41	120.94	111.37	120.23	99.65	96.10
122	162.04	160.83	168.10	165.42	147.61	121.53	104.27	122.94	99.67	96.64
123	160.67	162.17	168.48	160.23	142.57	121.53	111.29	122.73	95.41	97.07
124	159.69	158.04	170.59	164.56	142.74	121.33	113.41	120.69	97.86	96.14
125	163.60	166.11	172.67	165.49	149.24	121.33	102.04	119.18	100.00	98.80
126	163.60	160.76	168.25	163.96	157.09	122.31	115.28	122.75	97.93	99.80
127	160.86	156.03	168.27	166.35	155.03	122.31	113.04	121.69	99.84	100.14
128	163.41	162.56	172.42	164.26	159.25	122.31	112.68	120.38	98.57	102.54
129	163.80	155.90	168.83	163.29	156.11	123.48	113.75	121.61	96.67	100.71

130	172.41	165.36	168.52	167.06	167.99	110.18	111.26	104.40	103.68	101.39
131	172.41	164.24	167.42	168.46	170.16	110.18	109.60	104.71	105.43	101.36
132	166.73	160.68	168.19	166.93	170.83	109.00	110.94	104.68	105.37	101.67
133	169.47	169.48	172.72	167.72	168.54	109.00	109.26	103.78	106.47	102.03
134	171.43	168.19	168.80	168.08	167.91	109.59	109.98	103.43	104.07	100.69
135	171.82	164.87	168.09	167.07	169.05	109.98	107.97	104.56	106.91	101.11
136	166.54	165.52	168.14	169.25	169.91	109.00	108.73	104.45	107.01	99.82
137	169.28	170.09	172.43	169.74	172.79	109.00	105.65	104.06	105.91	102.35
138	171.62	165.35	169.36	167.86	168.59	109.39	108.82	103.46	106.94	102.05
139	171.04	165.03	170.59	169.48	165.35	109.00	110.44	104.12	106.88	103.20
140	171.04	166.65	166.81	167.52	166.67	109.39	106.28	104.47	105.08	103.22
141	165.17	165.91	165.59	169.29	165.26	108.22	110.38	104.23	106.57	103.55
142	168.69	171.84	172.66	168.99	166.51	108.22	109.98	102.92	107.22	102.80
143	171.04	167.71	170.08	169.37	163.67	108.81	106.01	104.40	105.93	103.67
144	171.04	165.12	167.71	169.26	165.26	109.20	107.91	104.44	106.22	103.51
145	165.95	165.43	168.18	169.36	164.59	108.22	111.40	104.59	106.44	103.46
146	168.10	169.11	172.34	168.53	166.51	108.22	111.48	103.77	105.81	102.71

147	170.65	169.47	168.97	169.29	165.26		108.61	110.35	104.30	106.57	103.55
148	173.19	168.41	169.05	158.08	147.05		104.50	99.07	102.86	89.82	86.01
149	174.17	167.68	168.84	162.12	160.26		104.70	94.15	104.89	87.80	92.61
150	174.17	161.94	168.56	163.15	152.84		103.91	98.87	103.15	95.32	88.09
151	172.99	165.49	169.84	158.65	144.65		103.91	94.31	104.47	91.39	84.89
152	174.36	162.88	169.71	151.59	142.25		103.91	100.90	102.39	82.84	83.62
153	171.04	166.05	163.16	161.32	137.26		105.09	93.87	104.71	85.14	79.46
154	172.80	160.20	167.67	153.29	134.17		105.09	89.26	104.29	83.80	77.84
155	175.34	171.30	170.77	154.59	134.57		105.09	96.96	103.85	84.66	78.15
156	175.34	163.77	165.66	152.10	136.78		105.09	96.18	103.63	82.30	80.05
157	161.25	160.54	168.99	166.14	170.83		96.09	94.02	100.51	90.79	95.34
158	158.90	155.35	161.59	165.48	172.86		96.28	95.68	97.37	90.77	97.83
159	161.25	162.82	167.08	165.32	169.54		96.87	98.22	96.03	91.13	95.96
160	161.25	158.19	165.83	166.57	172.01		96.48	97.32	97.63	92.44	98.94
161	159.88	159.94	164.55	166.53	166.82		96.48	93.97	96.58	92.65	92.03
162	161.64	161.72	169.04	165.08	171.27		96.67	97.51	96.35	90.56	98.57
163	161.64	161.32	164.93	164.68	166.30		96.48	91.97	96.88	91.13	91.62

164	159.49	156.96	166.40	164.08	164.28	96.09	95.88	96.34	90.88	92.40
165	160.86	158.21	167.66	165.42	171.96	96.87	95.08	99.77	88.07	97.86
166	165.56	159.45	165.04	151.05	153.41	95.11	96.19	95.85	82.80	93.24
167	164.58	152.77	160.96	167.88	167.99	95.11	93.86	95.51	91.25	96.79
168	166.54	162.85	168.44	158.16	166.89	95.11	96.45	95.49	85.99	98.15
169	166.54	157.92	163.07	168.07	159.02	95.30	91.77	95.00	92.92	88.62
170	165.75	157.31	165.90	165.06	148.01	95.11	86.60	103.92	90.86	87.43
171	166.14	159.03	167.94	164.53	156.96	95.30	92.05	94.61	92.20	90.86
172	166.14	156.98	163.74	167.26	167.30	94.72	91.57	93.40	90.99	94.61
173	164.97	159.10	164.26	165.47	153.90	94.13	96.66	94.26	90.94	88.76
174	168.69	131.61	168.75	169.22	167.96	99.61	69.33	103.50	108.21	101.52
175	173.78	171.20	171.83	167.45	168.41	101.37	100.93	104.11	102.17	99.88
176	173.78	164.29	168.85	166.58	161.94	101.37	98.72	104.60	102.51	91.59
177	170.45	166.96	167.50	167.66	166.59	100.78	91.97	104.74	102.45	96.96
178	173.58	165.71	172.61	167.19	168.93	100.78	91.20	103.97	100.82	100.52
179	173.58	164.56	168.29	167.46	165.34	101.57	95.70	103.76	102.51	95.48
180	172.41	168.64	168.41	167.95	169.80	101.37	91.63	105.14	101.83	101.46

181	170.06	167.20	167.81	167.04	168.87	101.37	95.25	104.30	100.09	101.08
182	173.97	170.78	171.55	167.12	169.15	100.78	96.01	104.28	100.21	100.26
183	173.97	163.68	168.30	166.78	167.56	100.98	100.87	104.57	100.16	99.15
184	169.86	164.70	168.60	168.94	165.48	100.78	96.62	103.72	106.67	95.48
185	173.19	170.45	172.61	169.13	166.27	100.78	100.47	102.05	106.14	97.61
186	173.19	167.62	168.42	168.96	164.53	101.17	99.69	104.24	106.80	95.52
187	172.99	166.99	168.28	168.99	164.26	100.98	99.34	100.99	106.76	95.36
188	170.06	166.40	169.64	169.13	166.27	100.98	100.77	102.08	106.14	97.61
189	172.80	168.86	171.08	168.25	166.02	100.98	102.30	104.53	105.57	96.07
190	172.80	168.44	169.28	169.40	169.05	100.59	98.73	104.00	107.99	97.48
191	171.43	167.49	169.37	169.46	169.83	99.80	100.72	102.77	107.29	98.11
192	169.86	168.54	170.16	168.89	164.29	99.80	100.64	103.01	106.21	95.39
193	169.08	167.12	168.33	169.02	173.16	98.24	101.75	104.59	106.88	101.39
194	167.71	166.56	169.21	169.28	171.09	98.24	103.52	104.24	106.73	99.18
195	166.34	165.80	168.81	168.52	172.20	98.24	97.93	101.88	105.73	100.76
196	169.28	168.26	171.02	169.40	170.55	99.02	101.75	103.65	104.92	97.73
197	169.28	168.77	168.06	169.05	171.10	99.61	101.40	102.75	104.64	99.19

198	167.91	166.24	168.05	168.86	170.60	99.80	100.60	104.20	103.84	97.47
199	168.88	164.95	171.04	169.80	170.67	99.80	100.54	103.38	108.40	98.07
200	170.84	169.30	170.79	169.89	172.67	100.39	107.65	103.59	106.66	98.40
201	170.84	165.96	169.42	168.94	169.83	100.39	101.41	104.66	106.02	97.16
202	170.84	120.24	169.42	168.94	169.83	100.39	101.41	104.66	106.02	100.39
203	175.34	166.32	174.54	161.8	169.45	120.35	115.73	117.25	101.33	120.35
204	175.34	164.32	177.54	165.16	174.65	120.94	118.2	117.5	108.18	120.94
205	171.23	165.4	172.43	166.56	169.43	120.55	120.19	118.88	109.94	120.55
205	175.34	170.4	173.26	166.43	171.11	120.55	115.05	118.71	113.92	120.55
206	176.13	165.4	175.68	166.36	171.46	122.5	117.29	117.6	110.82	122.5
207	176.13	170.12	175.45	166.7	171.24	122.11	119.13	120.78	109.13	122.11
208	171.04	175.5	170.5	166.11	171.29	120.94	117.52	117.5	110.96	120.94
209	176.32	170.34	176.3	170.45	171.98	120.94	116.35	122.18	111.24	120.94
210	176.32	178.34	176.42	170.43	170.45	100.39	101.41	104.66	106.02	100.39
211	173.97	170.78	171.55	167.12	169.15	100.78	96.01	104.28	100.21	100.26
212	173.97	163.68	168.30	166.78	167.56	100.98	100.87	104.57	100.16	99.15
213	169.86	164.70	168.60	168.94	165.48	100.78	96.62	103.72	106.67	95.48

214	173.19	170.45	172.61	169.13	166.27	100.78	100.47	102.05	106.14	97.61
215	173.19	167.62	168.42	168.96	164.53	101.17	99.69	104.24	106.80	95.52
216	172.99	166.99	168.28	168.99	164.26	100.98	99.34	100.99	106.76	95.36
217	170.06	166.40	169.64	169.13	166.27	100.98	100.77	102.08	106.14	97.61
218	172.80	168.86	171.08	168.25	166.02	100.98	102.30	104.53	105.57	96.07
219	172.80	168.44	169.28	169.40	169.05	100.59	98.73	104.00	107.99	97.48
220	171.43	167.49	169.37	169.46	169.83	99.80	100.72	102.77	107.29	98.11

Table A-2 – Systolic blood pressure estimation results for 22 individual patients.

Patient #	Raw Signal		PCA from Raw signal		21 Feature Extraction		21 Feature Extraction + PCA	
	ME/Patient	STDE/Patient	ME/Patient	STDE/Patient	ME/Patient	STDE/Patient	ME/Patient	STDE/Patient
1.	3.11	7.42	-6.52	2.34	-1.85	4.23	2.47	6.86
2.	2.62	2.96	-0.5	3.40	8.90	4.03	15.44	9.57
3.	6.49	3.34	5.42	2.17	12.36	7.14	18.06	13.62
4.	3.73	7.98	-0.08	2.03	2.81	5.86	9.21	7.59
5.	0.12	2.54	-3.57	2.00	5.31	2.17	9.00	9.93
6.	3.52	2.63	-0.05	4.11	11.93	2.22	-0.31	2.75
7.	3.33	4.46	-2.32	2.08	-4.44	2.21	-1.46	2.40
8.	-0.98	3.75	-4.81	1.46	-3.52	1.48	3.12	6.19
9.	11.39	3.11	12.24	3.50	20.98	2.88	16.45	3.23
10	6.94	7.07	1.50	3.52	4.18	2.44	0.02	2.33
11	4.92	6.66	1.23	3.97	8.47	5.59	4.61	3.73
12	-4.65	2.62	-5.02	3.12	-6.37	9.00	-4.10	5.29
13	-2.07	3.60	6.72	4.34	1.40	3.19	-11.01	5.78
14	-4.13	3.13	-0.88	3.10	-1.93	2.40	-1.16	3.55
15	-2.95	4.55	-1.02	3.66	-3.47	6.76	-8.50	9.04
16	-5.79	4.84	-1.42	6.11	-8.95	12.83	-16.96	24.06

17	-4.40	4.16	2.35	4.15	0.35	6.67	0.35	9.65
18	-9.54	10.00	-2.13	2.25	-3.27	3.25	-5.64	4.36
19	-4.78	2.24	-2.73	1.85	-3.91	2.08	-5.54	2.38
20	-1.76	1.23	0.42	1.52	0.16	1.27	1.55	3.17
21	-10.46	14.75	-0.40	1.27	-7.11	3.84	-2.83	2.19
22	-4.29	6.48	-2.50	2.06	-4.20	2.14	-6.01	1.83

Table A3 – Diastolic blood pressure estimation results for 22 individual patients.

Patient #	Raw Signal		PCA from Raw signal		21 Feature Extraction		21 Feature Extraction + PCA	
	ME/Patient	STDE/Patient	ME/Patient	STDE/Patient	ME/Patient	STDE/Patient	ME/Patient	STDE/Patient
1.	6.45	7.15	-1.79	1.81	11.84	5.06	18.32	4.03
2.	1.85	1.55	-0.17	1.27	7.22	2.19	21.18	4.09
3.	3.42	2.03	3.45	1.13	5.27	2.30	20.00	4.59
4.	2.19	3.28	0.9	1.98	3.86	2.12	18.23	10.68
5.	0.28	1.70	-2.59	1.07	-2.102	2.31	15.45	3.36
6.	2.00	1.79	1.56	1.10	2.60	1.15	13.30	0.89
7.	1.14	2.29	0.43	1.24	2.12	2.16	8.70	1.45
8.	1.99	3.16	-2.12	1.81	0.97	1.71	11.85	1.68
9.	6.36	2.89	2.06	0.93	3.93	3.20	9.71	1.62
10	0.94	4.95	-0.83	1.11	4.80	2.73	10.23	5.71
11	1.92	4.44	-0.81	1.02	9.41	5.58	19.68	4.94
12	-2.34	3.65	-2.04	1.77	-8.85	9.54	-12.61	13.65
13	-9.89	5.54	-1.07	2.08	-21.80	5.70	-21.79	4.86
14	-0.59	1.77	-5.18	0.58	-3.35	1.19	-7.60	1.25
15	-1.30	4.60	-3.31	1.88	-5.49	5.84	-8.27	5.20

16	-5.72	5.81	0.10	1.82	-13.86	7.99	-14.18	13.01
17	-1.91	3.05	1.34	2.78	-6.12	3.05	-2.16	3.86
18	-7.12	9.08	2.11	1.99	0.36	3.53	-2.94	3.58
19	-1.93	2.37	2.54	1.27	3.71	3.26	-3.38	2.01
20	2.36	2.38	4.11	1.22	6.84	1.58	-0.72	2.32
21	-2.74	2.48	-0.99	3.22	-8.21	7.95	-0.32	1.02
22	-1.22	5.32	2.67	1.38	4.45	2.78	-3.35	2.06